

The University of San Francisco
**USF Scholarship: a digital repository @ Gleeson Library |
Geschke Center**

Master's Theses

Theses, Dissertations, Capstones and Projects

Spring 5-16-2014

Glass Foundation Chemosensor Synthesis and Functionality Analysis

Justin D. Dancer

University of San Francisco, jddancer89@gmail.com

Follow this and additional works at: <https://repository.usfca.edu/thes>

 Part of the [Analytical Chemistry Commons](#)

Recommended Citation

Dancer, Justin D., "Glass Foundation Chemosensor Synthesis and Functionality Analysis" (2014). *Master's Theses*. 191.
<https://repository.usfca.edu/thes/191>

This Thesis is brought to you for free and open access by the Theses, Dissertations, Capstones and Projects at USF Scholarship: a digital repository @ Gleeson Library | Geschke Center. It has been accepted for inclusion in Master's Theses by an authorized administrator of USF Scholarship: a digital repository @ Gleeson Library | Geschke Center. For more information, please contact repository@usfca.edu.

Glass Foundation Chemosensor Synthesis and Functionality Analysis

A Thesis Presented to the Faculty
of the Department of Chemistry
at the University of San Francisco
in partial fulfillment of the requirements for the Degree of
Master of Science in Chemistry

Written by:

Justin Dancer

Bachelor of Science in Chemistry

Saint Mary's College of California, Moraga, CA

07/30/2016

Glass Foundation Chemosensor Synthesis and Functionality Analysis

Thesis written by Justin D. Dancer

This thesis is written under the guidance of the Faculty Advisory Committee, and approved by all its members, has been accepted in partial fulfillment of the requirements for the degree of

**Master of Science
in Chemistry
at
the University of San Francisco**

Thesis Committee

Lawrence Margerum, Ph.D.
Research Advisor

William Melaugh, Ph.D.
Professor

Ryan West, Ph.D.
Assistant Professor

Marcelo Camperi, Ph.D.
Dean, College of Arts and Sciences

Acknowledgement

I would like to thank my research advisor Dr. Larry Margerum for his help and guidance throughout my years at USF. I very much appreciate all the time and effort he put into our research and thesis editing. He was easily approachable and was always available to answer questions. I want to thank Dr. Melaugh and Dr. West for taking the time to be my thesis readers. I also want to thank Deidre Shymanski for all of her hard work behind the scenes in the chemistry department. I want to thank my five lab mates Jon, Katie, Alicia, Clara, and Simon for making our lab not only a place for learning but a place for fun as well. I want to thank my fiancé Audrey for all her love, support, encouragement, and insight throughout the writing of this thesis. Lastly, I want to thank my family, especially my parents and grandparents, for their love and support before, during, and after this graduate school journey. They instilled in me the importance of education from a very young age and set the foundation for me to be able to succeed. I cannot thank you enough and I love you all very much.

Table of Contents

Introduction to Chemosensor Synthesis	1
1.1 Controlled Pore Glass	1
1.1.1 Background	1
1.1.2 Pore and Particle Size	2
1.1.3 Surface Chemistry	3
1.2 Dendrimers	4
1.2.1 Background	5
1.2.2 PAMAM Dendrimers	6
1.2.2.1 Initiator Cores, Branching Units, and Surface Groups of PAMAM Dendrimers 8	
1.2.2.2 Dendrimer Size	9
1.2.3 Dendrimer Macromolecular Reactions	10
1.3 Indicator Displacement Assay (IDA)	12
1.4 Research Goals	13
1.5 References	14
Chapter 2	16
Synthesis and Characterization of a Molecular Sensing Ensemble from a Controlled Pore Glass Foundation	16
2.1 Introduction	16
2.1.1 CPG Acid Cleaning	16
2.1.2 CPG Activation	17
2.1.2.1 CPG Activation via 1,1'-carbonyldiimidazole (CDI)	17
2.1.2.2 CPG Activation via 3-(Triethoxysilyl)propylsuccinic anhydride	18
2.1.3 PAMAM Dendrimer Coupling to Activated CPG	18
2.1.4 Functional Group Density Assays	19
2.1.5 PAMAM activation via CDI	20
2.1.6 Ligand Reactions to Immobilized PAMAM Dendrimers	20
2.1.6.1 Coupling of $N\alpha$, $N\alpha$-bis(carboxymethyl)-L-lysine	20
2.1.6.2 Coupling of Amino-functionalized Terpyridine (A-terpy)	21

2.1.7	Metal Chelation to the Ligands Coupled to CPG-G _x	22
2.1.8	Indicator Displacement Assays on the CPG-G _x -NTA/Terpy-M ²⁺ Ensemble.....	23
2.2	Experimental Section.....	24
2.2.1	Chemicals and Materials.....	24
2.2.2	Instrumentation.....	26
2.2.3	Procedures.....	26
2.2.3.1	Controlled Pore Glass (CPG) Cleaning.....	26
2.2.3.2	Activation of CPG.....	27
2.2.3.2.1	Activation with CDI.....	27
2.2.3.2.2	Activation with TESPSA.....	27
2.2.3.3	PAMAM Dendrimer Immobilization on Activated CPG.....	27
2.2.3.4	Lysine NTA and A-terpy Couplings.....	28
2.2.4	Characterizations.....	29
2.2.4.1	Amine Density on CPG: 4NB Assay.....	29
2.2.4.2	CDI Density on CPG: Imidazole Assay.....	29
2.2.5	A-terpy Synthesis.....	30
2.3	Results and Discussion.....	31
2.3.1	Surface Primary Amine Density Assay.....	31
2.4	Conclusion.....	33
2.5	References.....	35
Experimental: Synthesis, Methods, and Assays for Molecular Sensing Ensembles.....		36
3.1	Results and Discussion: Ensemble Characterization and IDAs.....	36
3.2	CPG-CDI-G _{3,4} -terpy-Cu.....	36
3.2.1	CDI Coupled to CPG.....	37
3.2.2	PAMAM Dendrimer Reactions to CPG-CDI.....	38
3.2.3	CDI Activation of CPG-G _{3,4}	40
3.2.4	A-terpyridine Activation of CPG-G _{3,4}	41
3.2.5	Copper Loading onto CPG-G _{3,4} -terpy Precursors.....	43
3.2.6	Indicator Displacement Assays for CPG-G _{3,4} -terpy-Cu.....	44
3.3.1	TESPSA Coupling to CDI.....	47
3.3.2	Dendrimer Modification of CPG-TESPSA.....	48

3.3.3 CDI activation to CPG-TESPSA-G ₃	48
3.3.4 Lysine-NTA Ligand Activation and Copper Loading to CPG-TESPSA-G ₃ ..	49
3.3.5 IDAs on CPG-TESPSA-G ₃ -NTA-Cu Chemosensors	49
3.4 Conclusion	52
3.5 References	54
Chemosensor Optimization and Other Future Research Areas	55
4.1 Introduction.....	55
4.2 Synthesis and Assay Optimization.....	55
4.2.1 TESPSA Usage and Proof of Coupling	55
4.2.2 Dendrimer Generation Usage on Future Chemosensors.....	56
4.2.4 Ligand Diversity	57
4.2.5 Dye Optimization	58
4.2.6 Additional Substrates for IDAs	60
4.3 Conclusions.....	61
4.4 References	63

Abstract

Chemosensors are created through a series of reaction steps on controlled pore class (CPG) and terminate with a Cu^{2+} metal binding site. Each monolayer of reactant insures that the metal binding site exposed to solution would serve as an indicator displacement assay (IDA) sensor. The purpose of this research is to create a molecular sensor with a high density of terminal metal sites to quantify bidentate substrates. To accomplish this, each synthetic step of the sensor is examined in order to test the effects of new linkers, ligands, and variously sized dendrimers to see if small structural changes could promote a higher density of terminal metal sites. For linkers, the results show that CDI and TESPSA are comparable in functionality, whereas the ligand, lysine-NTA outperforms an amino-functionalized terpyridine in metal chelation. For dendrimers, higher generation dendrimers lead to more terminal Cu^{2+} metal binding sites than lower generation dendrimers.

Chapter 1

Introduction to Chemosensor Synthesis

In this research, molecular sensing ensembles are created through a series of reaction steps on controlled pore glass (CPG). Each monolayer of reactant insures that the metal binding site exposed to solution would serve as an indicator displacement assay (IDA) sensor. The purpose of this research is to create a molecular sensor with a high density of terminal metal sites using dendrimers to quantify bidentate substrates. To accomplish this, each part of the sensor is examined in order to test the effects of new ligands, metals, and dendrimers that could promote a higher density of terminal metal sites. This chapter introduces the chemistry of the solid foundation CPG, polyamidoamine (PAMAM) dendrimers, and the IDA as a method to quantify dye and bidentate substrates in solution via color change.¹

1.1 Controlled Pore Glass

CPG serves as the foundation and starting point for the synthesis of a molecular sensing ensemble. CPG has a wide variety of uses from immobilization, affinity, and liquid chromatography, to other uses such as bioceramics and even catalysis.^{2,3,4,5} Other uses, chemical properties, and the physical nature of CPG will be discussed in this chapter.

1.1.1 Background

Controlled pore glass is a porous solid made from silicon dioxide. CPG has pores on its outer shell that can range from 2-300 nm.^{5,6} These pores dramatically increase the surface area of the glass beads allowing for more surface hydroxyl groups. The more surface hydroxyl groups on the CPG, the more potential reaction sites the foundation possesses. The pore size typically used in this research is 500 angstroms, or 50 nm and the overall size of the glass beads is 120-200 μm .

Since the purpose is to create a sensor with a high number of terminal metal sites, using the CPG with the smallest pore size maximizes the reactive potential of the foundation because a higher surface area leads to a more reactive CPG foundation.

CPG has numerous advantages over other types of organic foundations. The solid glass structure can withstand high pressures and collisions that could take place in a reaction vessel during a synthesis. CPG is also hard to break down chemically; organic solvents, along with concentrated acids and bases are used alongside CPG without altering its reactivity or destroying its foundation.⁶ CPG also has varying pore size, particle size, and functional groups. CPG, with its surface hydroxyl groups, activates via nucleophilic reactions making the modification of the foundation a less arduous task.

1.1.2 Pore and Particle Size

The synthesis of controlled pore glass allows the resulting beads to have similar pore sizes. CPG is made from a borosilicate material which, when heated, expels borates uniformly, creating small pore size distributions where most pores are within 10% of the mean pore diameter.⁶ Since the reactivity of the foundation directly affects the surface modification to create the chemosensor, it is necessary to know how many hydroxyl groups are on the surface and to use the maximum amount of hydroxyl groups possible to make the best monolayer modification. According to Millipore's website, the surface area and pore size relate as shown below in Table 1-1.

Table 1-1. Relationship of pore diameter on CPG to surface area⁶

Pore Diameter (nm)	Internal Surface Area (m ² /g)
7.5	340
17	150
24	110
35	75
50	50
70	36
100	25
140	18
200	13
300	9

As the pore diameter increases, the internal surface area decreases. This inverse proportionality means that a smaller pore diameter increases the foundation's reactivity. However, since the CPG is only the foundation, and many more monolayers are added throughout the synthesis, the pore size must not be too small or steric effects will start hindering the surface modification. In this research a pore diameter of 50 nm is the best compromise, since dendrimer diameters range up to 4.5 nm in this work.⁷ Like pore size, particle size also varies with different kinds of CPG. Typical meshes range from 74 μm to 200 μm .⁶ Larger CPG particles will have more surface area but will also weigh drastically more than smaller CPG molecules. Therefore, smaller CPG particles will have a higher surface area leading to more surface hydroxyl groups.

1.1.3 Surface Chemistry

Knowledge of the surface chemistry of a CPG molecule is very important since it is the foundation of the chemosensors created here. At temperatures between 25 and 190 °C there exist four different types of silanol groups on the CPG surface: isolated silanols, geminal silanols, vicinal silanols, and surface siloxanes as shown in Figure 1-1.⁸

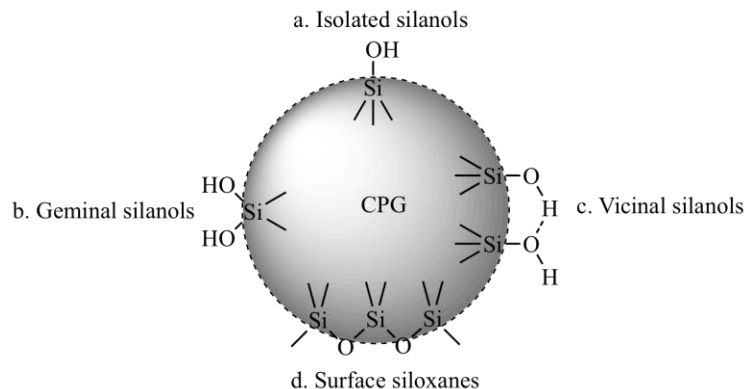


Figure 1-1. Different types of CPG surface groups. Reproduced from Zhuravlev.⁸

Three of the four types of groups already have hydroxyl groups on the surface of the CPG beads. The CPG surface must have these hydroxyl groups before subsequent syntheses take place. Concentrated nitric acid washing removes any potential organic impurities on the CPG but also provides protons in solution which transforms surface siloxanes into geminal silanols. This step insures that the CPG is pure and has the most possible hydroxyl groups on the surface before the first monolayer reaction.

1.2 Dendrimers

The covalent monolayers applied to CPG are macromolecular polyamidoamine (PAMAM) dendrimers and serve as the second monolayer, after the linker, on the ensemble. PAMAM dendrimers are useful because of their highly ordered three-dimensional arrangement and their functionality via terminal amine groups. This section introduces many properties of dendrimers including their structure, shape, branching, surface area, and reactivity in order to help the reader understand the properties and reaction mechanisms of these macromolecules.

1.2.1 Background

The earliest synthetic dendrimers were not created until the late 1970's and were not popularly used until after 1990.^{8,9} Dendrimers are composed of three regions depicted below in Figure 1-2.

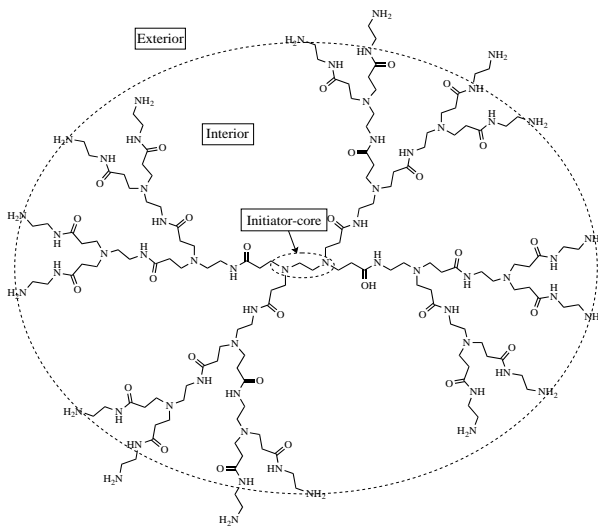


Figure 1-2. Picture of a generation 2.0 PAMAM dendrimer and its regions.

At the center of a dendrimer lies an initiator-core. Most PAMAM cores are n-alkyl diamines that terminate in primary amines. PAMAM dendrimer growth is achieved by the repeating of two alternating reactions. The first reaction is a Michael addition of the amino-terminated initiator core onto methyl acrylate, which results in an outer layer that is ester terminated. The second reaction is a coupling with ethylenediamine to generate the new amino-terminated surface, which results in a generation 0 dendrimer.¹⁰ Each time this pair of reactions takes place, a new “generation” forms. PAMAM dendrimers are classified by their generation number and typically are abbreviated as “G_x”, where X refers to the generation number. A G₁ dendrimer is created from a G₀ dendrimer by performing a Michael addition and then an ethylenediamine coupling. Half-

generation dendrimers are created by terminating a G_x dendrimer with a Michael addition, which yields a $G_{x.5}$ dendrimer. The second region of a dendrimer is its interior. The interior consists of all the atoms outside of the initiator core as the dendrimer increases in generation. The interior contains all the symmetric branches of the dendrimer structure that stem from the initiator core. The final region in a dendrimer is the exterior. The exterior is where the terminal functional groups lie and where further reactions take place. In PAMAM dendrimers, the exterior shell contains primary amines. Dendrimers can be as small as the core plus one interior reaction, G_0 , and as big as several generations. The company Dendritic Technologies[®] sells dendrimers as large as generation 10.¹¹

1.2.2 PAMAM Dendrimers

The terminologies for utilizing the PAMAM dendrimers are the interior of the dendrimer, which has tertiary amines as the branching unit for each generation, and the exterior, which consists of terminal amines that serve as a future reaction site for nucleophilic substitution. Starting at the initiator core, the only two possible reaction sites are at each terminal amine. When a generation increases, two more terminal amines exist at the end of each side of the newly formed generation zero PAMAM dendrimer. These amines then act as the only place for new reaction substitutions. This is the case for the synthesis of dendrimers as small as the initiator core to ones as large as generation 10. Figure 1.3 shows a synthesis up to generation 2.

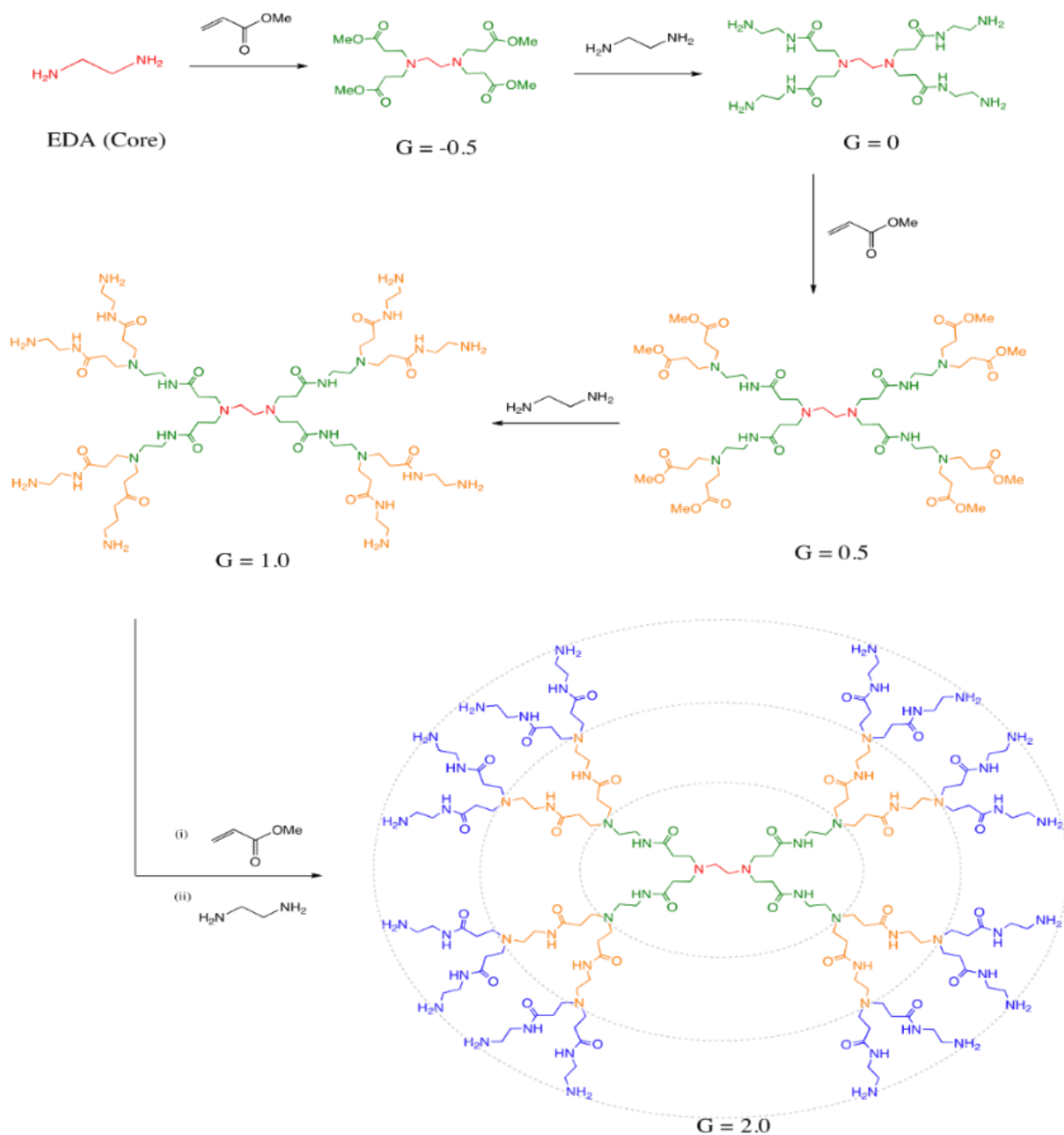


Figure 1.3. Dendrimer synthesis starting from initiator core to generation 2 PAMAM dendrimer.¹²

Since the only place for the dendrimer to increase in size is the same on both ends of the molecule, the resulting product has a uniform and symmetric structure. PAMAM dendrimers also have a high surface group functionality because of the terminal amines on the exterior. The number of surface amines doubles as a generation increases because when a new generation is added through substitution of terminal amines, two new terminal amines are produced at the new exterior. PAMAM dendrimers are available in many sizes, as in Table 1-2 in the next section, allowing the researcher a choice in the amount of reactivity and size of a dendrimer for a project. In this project, reactivity through terminal amine density is the most important aspect of a dendrimer. Dendrimers, with all their terminal amines, are polar molecules and when added to CPG make the modified ensemble more reactive, allowing more surface modification later in the synthesis than would be available to CPG alone. In other projects, researchers may use a dendrimer for its shape and size, where terminal amine density is not as important.¹³

The dendrimers in this research are typically G₃ and G₄ and purchased from either Sigma Aldrich or Dendritic Nanotechnologies Incorporated™. The dendrimers come as 10 to 20% by weight in methanol. As a pure substance, the dendrimers are viscous oils and stick to the sides of test tubes when the methanol is evaporates. The dendrimers are redissolved in DMSO, before they are added into a reaction vessel.

1.2.2.1 Initiator Cores, Branching Units, and Surface Groups of PAMAM Dendrimers

PAMAM dendrimers can have many different types of initiator cores. One can order cores such as ethylenediamine, diaminobutane, diaminohexane, diaminododecane, and even cystamine cores which have terminal amines branching out of a disulfide bond.¹⁴ The number of branching

units and the number of terminal amines differ only by two no matter how large the generation as shown in Table 1-2. One can calculate the number of surface groups on a dendrimer by the equation $2^{(n+2)}$, where n is the generation number. As generation increases, the number of surface functional groups doubles compared to the previous generation's amount of surface groups, giving the exponential function.

Table 1-2. The molar masses, number of branching units, and number of surface groups on ethylenediamine PAMAM dendrimers as a function of generation.¹⁵

Generation	Molar mass (g/mol)	Number of branching units	Number of surface groups
1.0	1502.03	6	8
2.0	3344.53	14	16
3.0	7029.52	30	32
4.0	14399.50	62	64
5.0	29139.47	126	128
6.0	58619.41	254	256
7.0	117579.28	510	512
8.0	235499.02	1022	1024
9.0	471338.51	2046	2048
10.0	943017.49	4094	4096

1.2.2.2 Dendrimer Size

Each time a dendrimer adds a generation, its molecular weight increases roughly by a factor of two. The higher generation a dendrimer gets, the more primary amines are exposed on the outer surface.¹⁶ These primary amines are what give dendrimers their reactivity and allow for their customization in many fields of research. PAMAM dendrimer structures, from G₃ and higher, are more disk-like than their lower generation counterparts, which are more spherical.¹⁷

In this research, the generation 3 PAMAM dendrimer, along with some generation 4 dendrimers, are studied. As PAMAM dendrimers increase in size, the price of the dendrimer

increases because the synthesis of a higher dendrimer generation takes longer, and requires more reagents and purification. Table 1.3 shows the prices of PAMAM dendrimers.

Table 1-3. Prices of PAMAM dendrimers with varying generation from Sigma Aldrich in 2014.¹⁴

Generation	Mass (g)	% Weight	Price (\$)	Price (\$) / g
3.0	5.00	20	272.50	272.50
4.0	2.50	10	220.00	880.00
4.0	10.0	10	667.00	667.00
5.0	5.00	5	237.00	948.00
6.0	5.00	5	383.00	1,532.00
7.0	2.50	5	593.00	4,744.00

1.2.3 Dendrimer Macromolecular Reactions

The two main areas where macromolecular interactions take place on dendrimers are through the primary amine groups and the interior tertiary amine groups. According to Maiti and coworkers, almost all of the primary amines on dendrimers are protonated by pH 7.4 and the majority of tertiary amines are protonated by pH 4 in aqueous solutions.¹⁶ Protonation of these amines will give the nitrogen atoms positive formal charge and cause an electrostatic repulsion against other positive atoms in the dendrimer structure. This effect can make a dendrimer increase its size and radius. Maiti also discovered that this increase happens for larger generations such as generation 4.0 through 8.0 but the lower generations are more rigid in structure.¹⁸

An article by Cakara aligns with Maiti's conclusion and reports microstate pKa data for the four primary amines and two tertiary amines of a G₀ dendrimer (Figure 1-3) quantified by titration curve fits and binding models; the results are in Table 1-4.¹⁹

Table 1-4. Comparison of macroscopic ionization constants pK_n of the PAMAM dendrimer G_0 from direct fit of the titration curves and calculated from the site binding model at different ionic strengths.¹⁹

n	0.1 M		0.5 M		1.0 M	
	Fit	Model	Fit	Model	Fit	Model
1	9.70	9.59	9.83	9.78	9.89	9.87
2	9.26	9.17	9.47	9.36	9.55	9.45
3	8.74	8.82	8.99	9.01	9.10	9.10
4	8.31	8.39	8.61	8.59	8.73	8.68
5	6.68	6.67	7.13	7.03	7.34	7.32
6	3.15	3.21	3.65	3.57	3.91	3.87

Maiti and Cakara both suggest that in a solution above pH 7, all four terminal amines are protonated whereas more acidic conditions are needed to protonate the tertiary amines. Cakara also performed the same experiment on a G_1 dendrimer with eight primary amines and six tertiary amines. In that experiment, the eighth terminal amine had a pK_a of 7.96, suggesting as dendrimer generation increases, the terminal amines require less acidic conditions to be deprotonated.¹⁹ As dendrimers increase in generation and have more terminal and tertiary amines, the pK_a values become harder to quantify. The pK_a of an amine becomes even more important when talking about nucleophilic substitution reactions of the dendrimer. If terminal amines are fully protonated then there is no nucleophilic lone pair of electrons available to attack an electrophile and ensure the reaction forms products. If a nucleophilic reaction cannot occur, dendrimer modification cannot occur and chemical modifications would produce no meaningful results. Therefore, running a nucleophilic reaction at a higher pH will render primary amines more nucleophilic thus creating a chemosensor with higher metal loadings.

1.3 Indicator Displacement Assay (IDA)

Indicator displacement assays originated with Inoue and are widely popularized by the Anslyn group.²⁰ One type of IDA is a chemical test where an unsaturated metal complex chemically coordinates or binds an indicator which is displaced by a substrate into an indicator solution and the absorbance difference used to calculate a concentration. There are two steps in an indicator displacement assay; the first step is the addition of a dye molecule onto the molecular sensor via metal chelation as shown in Figure 1.4.

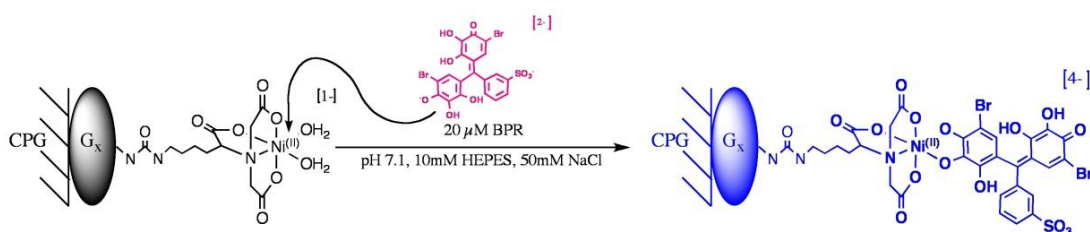


Figure 1.4. Picture of a CPG- G_x -NTA-Ni molecular sensing ensemble reacting with a bromopropyl red dye molecule to create the dye-loaded ensemble.²¹

The second step in an indicator displacement assay is the addition of a substrate that competes with the bound dye at the tethered metal ion site. If the substrate has better equilibrium binding properties than the dye, or is in much higher concentration, it displaces the dye as in Figure 1.5.

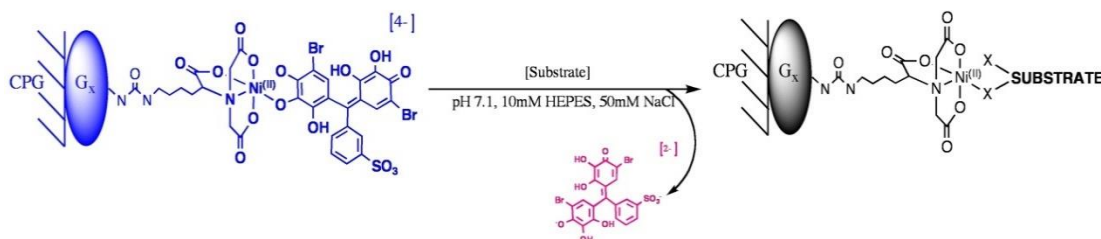


Figure 1.5. Picture of the introduction of a substrate to the molecular sensing ensemble and detachment of the dye molecule.²¹

From the change in solution absorbance, the amount of substrate bound to the sensor is quantified assuming a 1:1 exchange.

1.4 Research Goals

There are several goals to address as part of this research. The first is to create a working, highly sensitive ensemble, with CPG as a foundation, to perform IDAs on bidentate substrates. To have a highly sensitive ensemble, dendrimer functionality, ligand coupling, and metal loading must all be high. This means using a high dendrimer generation, creating ensembles with a suitable chelate, and loading high concentrations of a metal into the IDA site.

The second goal is to take a highly functional ensemble and ask what changes can be made to further increase its sensitivity. For example, what is the effect of changing dendrimer sizes on an ensemble? Also, which chelates, metals, and dyes will lead the most effective overall chemosensor?

The third goal is to detect and quantify biologically important molecules that potentially coordinate to the metal center via bidentate binding. There are many biological molecules worth sensing, many more than were tested in this work. Detecting and quantifying biological molecules is important for medicine, analytics, and the overall knowledge of chemical interaction.

1.5 References

1. Nguyen, B. T.; Anslyn, E. V., "Indicator displacement assays." *Coord. Chem. Rev.* **2006**, 250 (23,24), 3118-3127.
2. Robinson, P. J., Dunnill, P., Lilly, M. D., "Porous Glass as a Solid Support for Immobilization or Affinity Chromatography of Enzymes." *BBA Enzymology* **1971**, 242 (3), 659-661.
3. Miyake, K., "Determination of Partition Coefficients of Very Hydrophobic Compounds by High-Performance Liquid Chromatography on Glycerol-Coated Controlled-Pore Glass." *Journal of Chromatography A* **1982**, 240 (1), 9-20.
4. Hench, L., "Bioceramics: From Concept to Clinic." *Journal of the American Ceramic Society* **2005**, 74 (7), 1487-1510.
5. Kimtys, L., Aksnes, D., "Analysis of Pore Size Distribution by ^2H NMR." *Analyst* **2006**, 132, 148-152.
6. Millipore controlled pore glass (CPG) Media inorganic support for liquid chromatography and related application, EMD Millipore Coporation.
7. *Dendritech*. June 12, 2014. www.dendritech.com
8. Egon Buhleier, Winfried Wehner, Fritz Vögtle (1978). "'Cascade"- and "Nonskid-Chain-like" Syntheses of Molecular Cavity Topologies." *Synthesis* **1978**, 2, 155–158.
9. Hawker, C. J.; Fréchet, J. M. J. (1990). "Preparation of polymers with controlled molecular architecture. A new convergent approach to dendritic macromolecules." *J. Am. Chem. Soc.* **112**, 21, 7638.
10. Tomalia, Donald A.; Baker, H.; Dewald, J.; Hall, M.; Kallos, G.; Martin, S.; Roeck, J.; Ryder, J.; Smith, P., (1986). "Dendritic macromolecules: Synthesis of starburst dendrimers". *Macromolecules* **1986**, 19 (9): 2466–8
11. *Millipore*. June 12, 2014. www.millipore.com
12. Nicholson, J. W. (ED.) *The Chemistry of Polymers*; Royal Society of Chemistry: Cambridge, UK, 2006.
13. Esfand, R., Tomalia, D. A., "Poly(amidoamine) (PAMAM) Dendrimers: From Biomimicry to Drug Delivery and Biomedical Applications," *Drug Discovery Today*, vol. 6, no. 8, pp. 427-436, **2001**.
14. *Sigma Aldrich*. June 12, 2014. www.sigmaaldrich.com
15. Liu, S., Synthesis and study of various functional surfaces generated on PAMAM dendrimers immobilized controlled pore glass. M.S. Thesis, University of San Francisco, San Francisco, CA. **2013**.
16. Maiti, P., Cagin, T., Lin, S., and Goddard, W., "Effect of Solvent and pH on the Structure of PAMAM Dendrimers." *Macromolecules*. **2005**, 38, 979-991.
17. Pathak, S.; Singh, A. K.; McElhanon, J. R.; Dentinger, P. M., Dendrimer-Activated Surfaces for High Density and High Activity Protein Chip Applications. *Langmuir* **2004**, 20 (15), 6075-6079.
18. Holister, P., Vas, C. R., Harper, T., "Dendrimers: Technology White Papers." *Cientifica*. **2003**, 6, 6-15.

19. Cakara, D., Kleimann, J., Borkovec, M., "Microscopic Protonation Equilibria of Poly(amidoamine) Dendrimers from Macroscopic Titrations." *Macromolecules* **2003**, 36, 4201-4207.
20. Anslyn, E. V. "Supramolecular Analytical Chemistry." *J. Org. Chem.* **2007**, 72(3), 687-699.
21. Nguyen, B. T.; Anslyn, E. V. "Indicator Displacement Assays" *Coordination Chemistry Reviews* **2006**, 250, 3118-3127.

Chapter 2

Synthesis and Characterization of a Molecular Sensing Ensemble from a Controlled Pore Glass Foundation

2.1 Introduction

Controlled Pore Glass (CPG) serves as the foundation for the molecular sensing ensemble terminating in a chelated metal ion with exchangeable coordination sites. The CPG surface requires four monolayers to reach the desired metal site as in Figure 2-1.

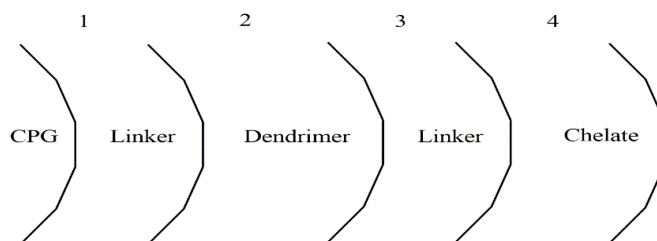


Figure 2-1. The four monolayers on CPG needed before the desired metal site.

Either 1,1'-carbonyldiimidazole (CDI) or 3-(triethoxysilyl)propylsuccinic anhydride (TESPSA), is the first monolayer applied and is a bifunctional linker between the CPG and the PAMAM dendrimer which is the second monolayer. The third monolayer is a CDI linkage between the terminal amines of the dendrimer and the metal ion organic chelating ligand, which is the fourth monolayer. Once the organic chelating ligand couples to the dendrimer, metal ions bind via the chelate, which is the site for the IDA.

2.1.1 CPG Acid Cleaning

Before activating the CPG, it must be cleaned and sanitized of any organic impurities by soaking in concentrated nitric acid. This insures that surface hydroxyl groups are created and no

impurities can alter the synthesis or prevent the maximum amount of hydroxyl groups from reacting with the linker.

2.1.2 CPG Activation

The CPG can be activated by one of two different molecules that perform the same function. Both CDI and TESPSA serve as a linker between the surface hydroxyl groups on the CPG surface and the amines branching from the dendrimer. These linkers will grant the two nucleophilic entities, the surface hydroxyl groups of CPG and the surface amines of the dendrimer, electrophilic regions that will serve as a tether to each other.

2.1.2.1 CPG Activation via 1,1'-carbonyldiimidazole (CDI)

The activation of CPG via CDI follows the work of Pathak.¹ CDI has a carbonyl site where a nucleophile can attack and displace an imidazole group into solution. The first reaction of the ensemble synthesis is the attack of a surface hydroxyl group of the CPG to the carbonyl carbon of the CDI, displacing a single imidazole group. In the second reaction, an amine from the dendrimer attacks the carbonyl and displaces the second imidazole group resulting in the CPG-CDI-G_x component of the ensemble as shown in Figure 2-2.

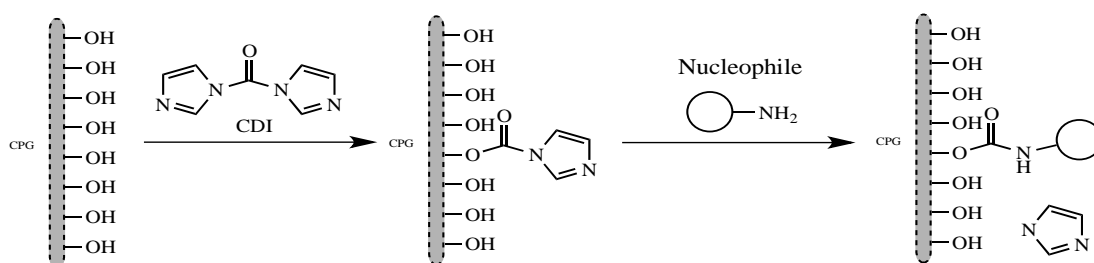


Figure 2-2. Reproduced from Stollner and Scheller.² Shows the binding of CDI to CPG and a terminal amine to CDI.

2.1.2.2 CPG Activation via 3-(Triethoxysilyl)propylsuccinic anhydride

The second way to link the dendrimer to the CPG foundation is via TESPSA as first published by Katzur who used TESPSA to connect dendrimers to silica wafers.³ The ethoxysilyl portion of TESPSA is the first nucleophilic substitution region as it reacts with the hydroxyl group from the CPG via displacement of an ethoxy group resulting in the first linkage as in Figure 2-3.

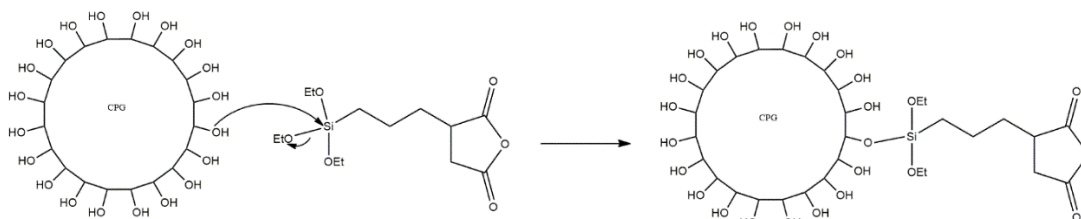


Figure 2-3. Nucleophilic substitution reaction between CPG and TESPSA

The second linkage from the dendrimer's amine happens at the carbonyl group in the succinic acid region. The amine attacks the carbonyl, which opens the succinic ring and results in a CPG-dendrimer covalent linkage.

2.1.3 PAMAM Dendrimer Coupling to Activated CPG

The terminal amines for PAMAM dendrimers of generation 3.0 and 4.0 are the nucleophiles that attack the electrophilic CDI monolayer on the CPG. CPG has a reasonably high number of hydroxyl groups at 4.6 ± 0.5 OH/nm², which suggests high functionality.⁴ TESPSA activation creates larger spacing from the surface than CDI that may reduce steric strain and increase the number of reaction sites. This is one hypothesis to be tested.

2.1.4 Functional Group Density Assays

Since these monolayers are added to improve the overall functionality of CPG, it is important to quantify all terminal reaction sites. The CDI assay quantifies imidazole groups after step one via hydrolysis, which releases imidazole into solution.² The free imidazole is compared to a calibration curve of imidazole absorbance at 208 nm versus known concentrations.

Concentration quantification of any available terminal amine groups on the surface was adapted from Moon.⁵ A sample reacts with 4-nitrobenzaldehyde (4NB) such that the terminal amine attacks the carbonyl carbon of 4NB forming an imine as shown in Figure 2-4.⁵

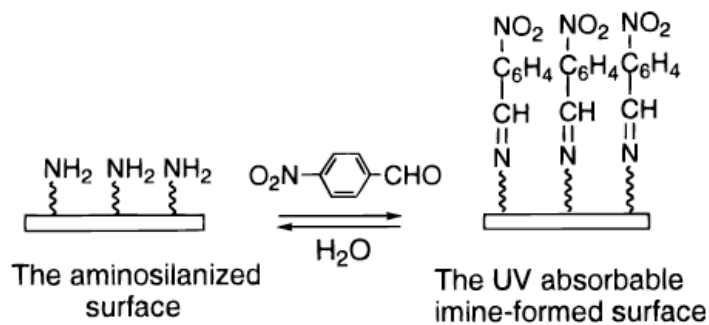


Figure 2-4. Reproduced from Moon.⁵ Nucleophilic amine attack on an aldehyde to form an imine.

After washing, the imines are hydrolyzed back into the terminal amine CPG and free 4NB. An external calibration curve of 4NB absorbance at 208 nm and the concentration of 4NB are used for calculations. Since the relationship of 4NB to terminal amines is one to one, the concentration of available terminal amines is equal to the concentration of 4NB with the assumption of completely reversible reactions.

2.1.5 PAMAM activation via CDI

After showing that PAMAM dendrimers anchor to the CPG surface, another CDI monolayer is added before a ligand can be coupled to the dendrimer.

2.1.6 Ligand Reactions to Immobilized PAMAM Dendrimers

Two chelating ligands are used for this research, which strongly chelate metal ions. The first is $N\alpha, N\alpha$ -bis(carboxymethyl)-L-lysine (Lysine-NTA), which is an analog of nitrilotriacetic acid, and the second is aminofunctionalized terpyridine (A-terpy).

2.1.6.1 Coupling of $N\alpha, N\alpha$ -bis(carboxymethyl)-L-lysine

Lysine-NTA synthesis and dendrimer coupling was adapted from Cheng-Chi Chang.⁶ The lysine-NTA molecule is similar to a nitrilotriacetic acid chelation while a reactive amine on the other side serves as the nucleophilic site for CPG reactions shown in Figure 2-5.

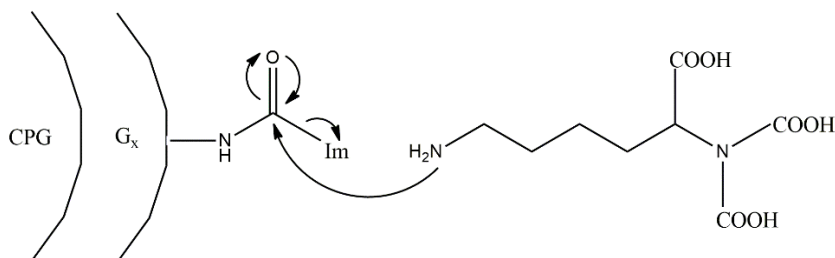


Figure 2.5. Lysine NTA amine attacking the carbonyl carbon of the linker to couple the chelate to modified CPG.

Lysine NTA is useful because it has both the chelation properties necessary to bind a metal ion and a nucleophilic site for coupling to the modified surface. Lysine NTA is also commercially available from Sigma Aldrich for \$193.50 / gram.⁸ Table 2.1 shows the binding constants for NTA with certain metal ions.

Table 2-1. Binding constants of various transition metals with NTA.⁹

Metal Ions	LogK/M^{-1} $\text{M}^{2+} + \text{NTA}^{3-} \rightarrow [\text{M}(\text{NTA})]^{-}$
Mn(II)	7.44
Fe(II)	8.84
Co(II)	10.6
Ni(II)	11.26
Zn(II)	10.45

2.1.6.2 Coupling of Amino-functionalized Terpyridine (A-terpy)

Like lysine-NTA, amino-functionalized terpyridine has one end for chelation via the three pyridine nitrogens of the aromatic rings, but also has a nucleophilic tail terminating with an amine.

Figure 2.6 shows this ligand after coupling to the dendrimer on CPG.

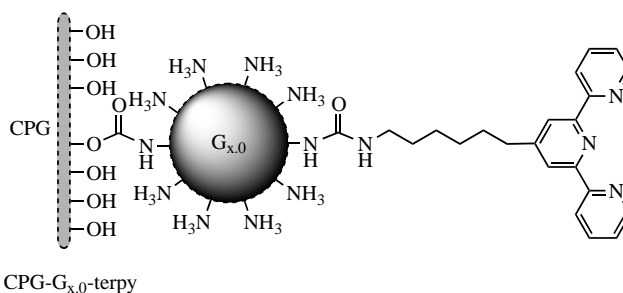


Figure 2.6. Picture of a CPG- $G_{x,0}$ -terpy molecule linked via CDI activation of CPG. Picture drawn by Sandy Liu.⁷

This amino-functionalized terpyridine is not commercially available and the synthesis is adapted from Schubert et al. and beginning with commercially available 4'-chloro-2,2':6',2''-terpyridine.¹⁰ Binding constants for terpyridine with several metal ions are shown in Table 2.2.

Table 2-2. Binding constants of various transition metals and terpyridine¹¹

Metal Ions	LogK/M ⁻¹ M ²⁺ terpy → [M(terpy)] ²⁺
Mn(II)	4.4
Fe(II)	7.1
Co(II)	8.4
Ni(II)	10.7
Zn(II)	6.0

2.1.7 Metal Chelation to the Ligands Coupled to CPG-G_x

The modified CPG is transferred to a plastic Poly Prep[®] chromatography column (PPCC) while a 5 ppm solution of a desired metal, usually Ni²⁺ or Cu²⁺, flows through the ensemble and out the bottom of the column. The process is controlled by a pump and fraction collector. Early in the flowing process, the solution passes through the modified CPG where the ligand starts to chelate the metal in solution. Subsequently, the 5 ppm metal solution saturates the ensemble and no longer loses any of its metal ions to chelation, therefore eluting a 5 ppm solution of metal ion. Fractions collected produce a “breakthrough curve” of ppm vs. metal ion eluted volume of 5 ppm solution passed. This curve is similar to a pH curve; initially the ppm of the eluent is small, but as the chelating sites saturate there is a drastic increase in metal ion concentration, which levels out at about 5 ppm as in Figure 2-7.

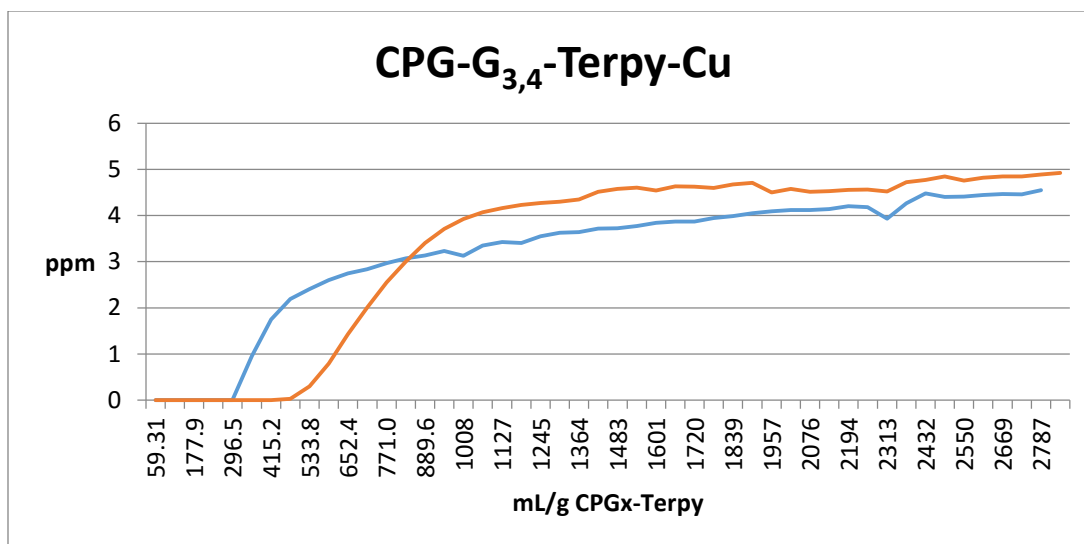


Figure 2-7. Graph of two breakthrough curves of different generation dendrimers with terpy as the chelate.

At this time, the resulting ensemble is buffer washed to remove any soluble metal ions that are flowing around the chemosensor. The result is that the chemosensor is loaded and ready for indicator displacement assays.

2.1.8 Indicator Displacement Assays on the CPG-G_x-NTA/Terpy-M²⁺ Ensemble

An indicator displacement assay (IDA) is an assay where a metal ion bound indicator is exposed to a newly introduced substrate that competes for the open metal site via an exchange mechanism. Initially, the chemosensor is placed into a screw-cap vial. An aliquot of dye solution, typically pyrocatechol violet, is added to the vial containing the chemosensor. The chelation of the dye to the metal ion is the first step of the IDA as in Figure 2-8.



Figure 2.8. A molecule of BPR chelating a nickel metal center of a modified CPG molecule.

The absorbance of the dye at 440 nm starts initially around 1.15. After 24 hours of exposure to the chemosensor, the dye absorbance decreases because some of the dye has chelated to the metal ion chemosensor decreasing the free dye concentration. An aliquot of a 100 mM substrate solution is added to the reaction vial for 24 hours. Usually the final absorbance increases because some substrate chelates to the metal site, kicking off the dye into solution, which is a function of substrate concentration as in Figure 2.9.

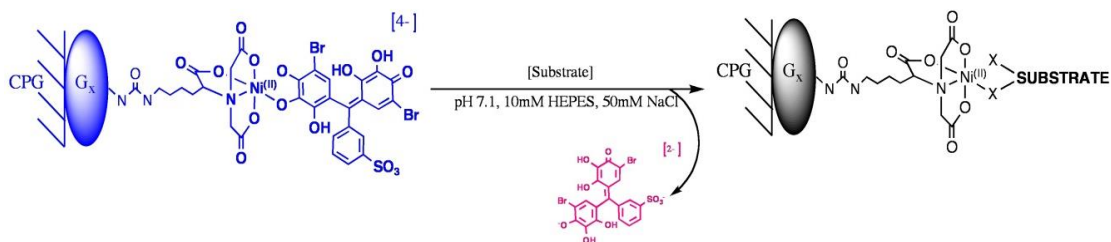


Figure 2.9. A substrate chelating a nickel metal center and kicking off the dye molecule.

2.2 Experimental Section

2.2.1 Chemicals and Materials

All the chemicals used in this research were purchased and used as received. The glassware were washed with soap and deionized water thoroughly unless the glassware was used to hold

metal ions. In this case, the glassware was soaked in a 1.0 M nitric acid bath for more than 24 hours and washed thoroughly with soap, followed by deionized water.

Chemicals: Nitric acid (68–70 % ACS reagent grade), acetic acid (glacial, ACS reagent grade), and methanol were purchased from Pharmco-Aaper. Hydrochloric acid (36.5-38.0 %, Baker analyzed ACS reagent), sodium phosphate dibasic anhydrous (USP/FCC, FW: 141.96), and triethylamine (TEA, FW: 101.19) were purchased from J.T.Baker. Sodium hydroxide (50 % by weight) was purchased from VWR. N α , N α -bis(carboxymethyl)-L-lysine hydrate (Lys-NTA, \geq 97.0 % (TLC), FW: 262.26), 1-1'-carbonyldiimidazole (CDI, reagent grade, FW 162.15), ethyl acetate (ACS reagent), dichloromethane (99.6%, ACS spectrophotometric grade, FW 84.93), N-hydroxysuccinimide (NHS, \geq 98 % FW 115.09), imidazole (anhydrous Grade I, crystalline, FW: 68.08), dopamine hydrochloride (FW: 189.64), L-alanine (Sigma grade, FW: 89.1), L-histidine (SigmaUltra, > 99 % (TLC) FW: 155.2), L-leucine (Sigma grade, FW:131.2), and pyrocatechol violet (Indicator grade, FW: 386.38) were purchased from Sigma Aldrich. Starburst Dendrimer in methanol generation 3 – diaminohexane core – amine surface (G_{5.0}, DNT 115, 20 % w/w, FW: 6,909), Starburst Dendrimers in methanol generation 4 - diaminobutane core – amine surface (G_{4.0}, DNT 106 10% w/w, FW: 14,215), and Starburst Dendrimers in methanol generation 4 – diaminobutane core – amine surface (G_{5.0}, DNT 106, 10 % w/w, FW: 28,826) were purchased from Dendritic Nanotechnologies Incorporated. TESPSA was purchased from J&K Scientific LTD. 4'-chloro2,2':6'2''-terpyridine (chloro-terpy, 98 %, FW: 267.72), 5-amino-1-pentanol (amino-pentanol, 97 %, FW: 103.17), 4-nitrobenzaldehyde (4NB, 99 %, FW: 151.12), and 6,7-dihydroxy-4-methylcoumarin (DHMC, 97 %, FW: 192.17) were purchased from Alfa Aesar.

Drisolv[®] p-dioxane anhydrous (1,4-dioxane, FW: 88.11) and Drisolv[®] methylsulfoxide anhydrous (DMSO, FW: 78.14) were purchased from EMD.

Materials: Controlled pore glass (CPG) CPG500B (CPG, mesh size 500 Å, pore size 74-125 µm, surface area 45.2 x 10¹⁸ nm²) was purchased from Millipore and Poly Prep[®] chromatography columns (PPCC) were purchased from Biorad Laboratories.

2.2.2 Instrumentation

The deionized water was purified by a SpectraPure[®] Reverse Osmosis & Deionization System equipped with a SpectraPure[®] BA-ICE-S Electronic ICE Controller. Mass measurements were conducted using a LabServe[™] Sartorius R160P analytical balance. UV-Vis measurements were performed on an Agilent 8453 UV-Visible Spectrophotometer equipped with an Agilent 89090 Peltier Temperature Controller. Spinning samples and solvent evaporations were made possible by the use of a Buchi Rotovapor[®] R-114 and mixing was done on a New Brunswick Scientific Reciprocal Water Bath Shaker model R76.

2.2.3 Procedures

2.2.3.1 Controlled Pore Glass (CPG) Cleaning

About 2.0 – 2.5 g of CPG beads were weighed into a round bottom flask with 50 mL of concentrated nitric acid. The flask was attached to a rotary evaporator slowly spinning in the 70 °C water bath for 3 hours under nitrogen atmosphere. The CPG beads were then filtered using a Kimax filter funnel and rinsed thoroughly with 3.0 L of deionized water. The pH of the washes were monitored using pH paper until they were neutral. The beads were then dried in an oven at 120 °C for 24 hours (usually the day before a reaction took place). The washed beads were cooled

and either stored in a PPCC inside a vacuum desiccator for future use, or reacted immediately with a tether to start the ensemble synthesis.

2.2.3.2 Activation of CPG

There were two ways to activate CPG. The first was established in the Margerum group for linking two nucleophilic entities using 1,1'-carbonyldiimidazole. The second was one using a newly utilized linker, 3-triethoxysilylpropylsuccinic anhydride.

2.2.3.2.1 Activation with CDI

CDI was first dissolved in 50.0 mL of 1,4-dioxane, such that the resulting solution was 0.2 M, before it was added to a 100 mL round bottom flask with 2.0 – 2.5 g of clean and dry CPG beads. The reaction spun slowly on a rotary evaporator at room temperature for 24 hours under a constant flow of nitrogen gas. The CPG-CDI were filtered through a Kimax medium glass filter funnel and rinsed with 100 mL of 1,4-dioxane for each gram of CPG reactant. The filtered product was vacuum dried and stored in a PPCC in a vacuum desiccator.

2.2.3.2.2 Activation with TESPSA

The procedure for reacting TESPSA with CPG was adopted from Katzur.³ A mixture of 1.6 mmol/L TESPSA and 4.8 mmol/L acetic anhydride in toluene was added to a round bottom flask with 2.0 g CPG inside. The reaction was heated at 100 °C for 30 minutes in an oil bath and then to 130 °C for an additional 10 minutes. The product was washed with toluene to remove excess acetic anhydride and TESPSA, and then dried in a vacuum desiccator.

2.2.3.3 PAMAM Dendrimer Immobilization on Activated CPG

The activated CPG-CDI and CPG-TESPSA were weighed into 20 mL disposable scintillation vials. A stoichiometric amount of PAMAM dendrimer, dissolved in methanol as

received from Dendritic Nanotechnologies Inc., was put in a test tube and a stream of nitrogen gas was used to evaporate the solvent. The resulting oil was dissolved in 20.0 mL of anhydrous DMSO and added to the scintillation vial. The scintillation vial was then filled with nitrogen gas, capped, sealed with electrical tape, and then spun on the rotary evaporator for 72 hours. This sample of CPG-CDI/TESPSA-G_x was added to a PPCC and rinsed with 75.0 mL of anhydrous 1,4-dioxane. The modified particles were vacuum dried and stored in a desiccator.

2.2.3.4 Lysine NTA and A-terpy Couplings

Another monolayer of CDI was added to CPG-Linker-G_x before the ligand was coupled. This allowed the two nucleophilic entities to couple to each other via the carbonyl.

CPG-Linker-G_x reaction with CDI: Enough CDI was dissolved in 20.0 mL of 1,4-dioxane in order to form a 0.20 M CDI solution. This solution was poured into a 20 mL scintillation vial along with 750 mg of CPG-Linker-G_x and the reaction rotated on a rotary evaporator for 24 hours at room temperature. The beads were filtered through a PPCC, rinsed with 75.0 mL of anhydrous 1,4-dioxane, vacuum dried, and stored in a desiccator.

CPG-Linker-G_x reactions with lysine-NTA or A-terpy: Appropriate amounts of lysine-NTA or A-terpy along with NHS and TEA were added to 20.0 mL of DMSO. The mixture was added to a scintillation vial with the weighed ensemble. The reaction spun on the rotary vaporizer for 72 hours at room temperature. The sample was poured into a PPCC and rinsed with 100.0 mL of anhydrous DMSO before being vacuum dried and stored in a desiccator.

2.2.4 Characterizations

2.2.4.1 Amine Density on CPG: 4NB Assay

The purpose of this assay was to calculate the available surface amine groups on a dendrimer surface. There were three solutions made: 0.10 M 4NB solution dissolved in methanol, 0.2 % (v/v) acetic acid solution dissolved in deionized water, and a 1.00 mM 4NB solution dissolved in the 0.2 % (v/v) acetic acid solution. A small sample of CPG-Linker-G_x was weighed into a 20 mL scintillation vial (typically 10 mg) with 20 mL of 0.10 M 4NB solution in methanol. This reaction was rotated for 24 hours at room temperature. The product was washed with anhydrous methanol in a PPCC and vacuum dried in a desiccator. The dried and filtered product was separated into three 20 mL scintillation vials and 15.00 mL of the 0.2 % (v:v) acetic acid solution was pipetted into the vials and shaken for 4 hours at room temperature.

The 1.0 mM NB in 0.2 (v:v) acetic acid solution was used to make a calibration curve. Volumes of 10 μ L were digitally pipetted into a quartz cuvette already filled with 2.500 mL of 0.2% (v:v) acetic acid solution. The cuvette was shaken after each aliquot added to ensure the solution matrix was homogeneous before taking the absorbance of the sample at 268 nm. A calibration curve of absorbance vs. 4NB concentration was created and the total volume was corrected to ensure the molarity was correct. Once the calibration curve was produced, the sample solutions' absorbance values were taken and their concentrations were calculated.

2.2.4.2 CDI Density on CPG: Imidazole Assay

The CDI assay was used to quantify how many CDI molecules reacted with the CPG or the dendrimer after a second CDI layer was added (CPG-CDI and CPG-CDI-G_x-CDI). A 5.0 mM sodium phosphate dibasic solution of pH 10.0 was prepared along with a 10 mM imidazole

solution dissolved in 5.0 mM sodium phosphate dibasic solution. A sample of the imidazole terminated CPG was weighed in a 20 mL scintillation vial and 15.00 mL of 5.0 mM sodium phosphate dibasic solution was pipetted into the vial. The samples were shaken at 50 °C for 4 hours in a water bath. The samples were cooled to room temperature and their absorbance values taken at 208 nm. About 10 µL per aliquot of the 10 mM imidazole solution was pipetted into 2.000 mL of 5.0 mM sodium phosphate dibasic solution. A calibration curve was plotted from these data and used to calculate the concentration of the CPG modified samples.

2.2.5 A-terpy Synthesis

Solid potassium hydroxide (KOH) was ground, using a mortar and pestle, and dried overnight in an oven at 100 °C. Then, 0.60 g KOH powder and 0.200 g (1.94 mmol) 5-amino-1-pentanol were transferred to a 50 mL round bottom flask along with 25 mL DMSO. This solution was mixed on a rotary evaporator for 30 minutes in an 80 °C water bath while the solution was being purged by nitrogen gas. Then, 0.500 g (1.87 mmol) of 4'-chloro-2,2':6'2''-terpyridine (chloro-terpy) was added to the round bottom flask. The reaction was spun on the rotary evaporator for 4 hours, under nitrogen gas, in a water bath at 70 °C. The reaction solution was quantitatively transferred to a separatory funnel using 200 mL of deionized water. Three volumes of 20.0 mL of dichloromethane were added to separate the organic layer from the aqueous layer. The organic layer was isolated and dried using sodium sulfate and gravity filtered into a preweighed pear-shaped flask. The flask was connected to a rotary evaporator to remove the solvent. The product's color was a light orange-yellow solid. The product was recrystallized with ethyl acetate and stored in the refrigerator. The crystals were collected by vacuum filtration on a Buchner funnel, washed with DMSO, and stored in a scintillation vial in a desiccator. The yield

was 0.93315 g, a 74.7% yield based on the limiting reagent. NMR data of the results show two aromatic regions from the starting material 4'-chloro-2,2':6'2''-terpyridine and the A-terpy product. The chloroterpy aromatic protons were more deshielded due to the chlorine and ranged from δ 8.5 to 9.0, whereas the A-terpy ranged from δ 7.5 to 8.2. A peak at δ 4.3 represented the CH₂ group bonded to the oxygen on 5-amino-pentanol portion of the A-terpy. The integration of the δ 4.3 matched that of an aromatic hydrogen in a 1:1 ratio, which supported the idea that they were connected on the same molecule A-terpy. However, the integration of the starting material peak aromatic region was three times larger than the A-terpy aromatic region. Therefore, the final A-terpy product was only about 30% pure.

2.3 Results and Discussion

As the size or generation of dendrimer immobilized onto CPG increased, the functional group assays showed increasing surface imidazole groups in the CDI assays and more primary amines in the amine density assays. This result is strong evidence of successful dendrimer immobilization and is not surprising since the terminal primary amines increases as the generation of dendrimer increases.

2.3.1 Surface Primary Amine Density Assay

After the dendrimers were added to the CPG foundation, the amount of terminal amines were quantified using an amine density assay adapted from Moon *et al.*⁵ The method relies on the reversible addition of 4NB to a sample of dendrimer coated CPG, which forms an imine between the two entities. Once enough time passed for reaction with 4NB, the sample was washed and reacted with 0.2 % (v:v) acetic acid solution to cleave the 4NB back into solution and absorbance values from UV-Vis gave quantification using a calibration curve. There were some assumptions

made about this assay. It was assumed that all the 4NB that reacted with the terminal amines were also cleaved back into solution with the dilute acetic acid. It was also assumed that the 4NB and a terminal amine reacted in a 1:1 ratio.

The amine densities are reported in units of $\mu\text{mol NH}_2/\text{g CPG}$. The calculation for $\mu\text{mol NH}_2/\text{g}$ is shown in Equation 2-1.

$$\mu\text{mol NH}_2/\text{g CPG} = \frac{[\text{4NB}] * V * 10^6}{\text{g CPG}} \quad \text{Equation 2-1}$$

V is volume of the sample and then multiplied by 10^6 is the change from moles to μmol . An example spreadsheet calculation of the $\mu\text{mol NH}_2/\text{g}$ is shown in Table 2-3 below. For the new TESPSA linker method, the main sample is split into three smaller samples labeled A, B, and C respectively. The mass values vary but the deviation in $\mu\text{mol NH}_2/\text{g CPG}$ is small.

Table 2-3. Amine density assay results of a generation 3 dendrimer modified CPG beads linked with TESPSA and washed with HEPES buffer.

Sample	Mass (g)	Volume (mL)	Abs.	4NB (moles)	$\text{NH}_2/\text{g CPG}$ (μmol)
CPG-TESPSA-G ₃ A	0.02686	15.00	1.2430	1.628E-06	60.62
CPG-TESPSA-G ₃ B	0.01060	15.00	0.45047	6.116E-07	57.70
CPG-TESPSA-G ₃ C	0.01107	15.00	0.47743	6.455E-07	58.32
					59 ± 2

Sandy Liu, along with other researchers before her, showed that amine density increases on CDI activated CPG as the generation of dendrimer increases.⁷ This is consistent with the increasing terminal amine count with increasing dendrimer generation. For comparison, amine assays were

performed with dried and purified CPG-TESPSA-G₃ along with HEPES buffer washed CPG-TESPSA-G₃. Table 2-4 shows the results of an amine density assay with same three samples of CPG-TESPSA-G₃, but without buffer wash.

Table 2-4. Amine density assay of CPG-TESPSA-G₃ without HEPES buffer washing

Sample	Mass (g)	Volume (mL)	Absorbance	4NB (moles)	NH ₂ /g CPG (μmol)
CPG-TESPSA-G ₃ A	0.00725	15.00	0.078105	1.831E-07	25.25
CPG-TESPSA-G ₃ B	0.00500	15.00	0.046771	1.400E-07	28.00
CPG-TESPSA-G ₃ C	0.00567	15.00	0.047055	1.404E-07	24.76
					26 ± 2

These data imply that a HEPES buffer wash on dendrimer modified CPG increases the availability of reactive dendrimer terminal amines on the CPG. For the imine formation to occur in the assay, the lone pair on the amine must be available for nucleophilic attack. If the amine is protonated and has a positive charge, the amine will not have a lone pair to perform the attack. The HEPES buffer wash must change the surface charge of some of the terminal amines from positive to neutral by pulling off an extra hydrogen from a positively charged terminal amine. This result needs to be tested over a broader range of dendrimer generations and trials to confirm the results.

2.4 Conclusion

The amine density assay is a good method to quantify surface amines on samples and thus predict their future reactivity and surface charge. The deviations between trials are low meaning the assay's precision is high ($\pm 2 \mu\text{mol NH}_2 / \text{g CPG}$). The assay gives quantitative information about synthetic efficiency and gives insight on potential future reactivity of the ensemble. Low amine density assays results typically lead to low chelate-metal loadings. This hinders IDA

performance because high amine density assays give higher metal loadings and larger spectroscopic changes in IDAs. Also, the new result of washing the samples with HEPES buffer further activates the terminal amines and increases sensitivity; however, this idea needs further testing to make sure the results are valid.

2.5 References

1. Pathak, S.; Singh, A. K.; McElhanon, J. R.; Dentinger, P. M., Dendrimer-Activated Surfaces for High Density and High Activity Protein Chip Applications. *Langmuir* **2004**, *20* (15), 6075-6079.
2. Stollner, D., Scheller, Frieder W., Warsinke, Axel, Activation of cellulose membranes with 1,1'-carbonyldiimidazole or 1-cyano-4-dimethylaminopyridinium tetrafluoroborate as a basis for the development of immunosensors. *Anal. Biochem.* **2002**, *304* (2), 157-165.
3. Katur, V., Eichler, M., Deigele, E., et. all., Surface-immobilized PAMAM-dendrimers modified with cationic or anionic terminal functions: Physiochemical surface properties and conformational changes after application of liquid interface stress. *J. Colloid Interface Sci.* **2012**, *366*, 179-190.
4. Zhuravlev, L. T., The surface chemistry of amorphous silica. Zhuravlev model. *Colloids and Surfaces A.* **2000**, *173* (1, 3), 1-38.
5. Moon, J. H.; Kim, J. H.; Kim, K.-j.; Kang, T.-H.; Kim, B.; Kim, C.-H.; Hahn, J. H.; Park, J. W., Absolute Surface Density of the Amine Group of the Aminosilylated Thin Layers:, A Ultraviolet, àVisible Spectroscopy, Second Harmonic Generation, and Synchrotron-Radiation Photoelectron Spectroscopy Study. *Langmuir* **1997**, *13* (16), 4305-4310.
6. Chang, C.-C., End-group Modifications to PAMAM Dendrimers Tethered on Glass Supports: Development of Indicator Displacement Assays (IDA) Based on Tethered Copper Chelates. M.S. Thesis, University of San Francisco, San Francisco, CA, **2009**.
7. Liu, S., Synthesis and study of various functional surfaces generated on PAMAM dendrimers immobilized controlled pore glass. M.S. Thesis, University of San Francisco, San Francisco, CA. **2013**.
8. *Sigma Aldrich*. August 18, 2014. www.sigmaaldrich.com
9. Furia, Thomas E. *Crc Handbook of Food Additives*. 2nd ed. Vol. 1. Boca Raton, Florida: CRC, **1975**.
10. Schubert, U. S.; Eschbaumer, C.; Hien, O.; Andres, P. R., 4-Functionalized 2,2':6',2"-terpyridines as building blocks for supramolecular chemistry and nanoscience. *Tetrahedron Lett.* **2001**, *42* (28), 4705-4707.
11. Shunmugan, R.; Gabriel, G.; Aamer, K; Tew, G; Metal-Ligand-Containing Polymers: Terpyridine as the Supramolecular Unit. *Macromol. Rapid Commun.* **2010**, *31*, 784–793.

Experimental: Synthesis, Methods, and Assays for Molecular Sensing Ensembles

3.1 Results and Discussion: Ensemble Characterization and IDAs

In this chapter, the quantifiable results using CPG-CDI-G_{3,4}-terpy-Cu and CPG-TEPSA-G₃-NTA-Cu as sensors are discussed. CDI, shown Figure 2-2 in Chapter 2, was reacted with CPG before a dendrimer coupled to the foundation. These dendrimers then coupled a ligand, which chelated copper ions. Each synthetic step gave an intermediate product that was analyzed by a CDI assay, amine assay, or breakthrough curve. CDI assays allowed the quantification of CDI coupled to the CPG foundation and to the dendrimer whereas the amine assay allowed the quantification of amine density once the dendrimer coupled to CPG. A breakthrough curve was produced to measure copper ions.

The indicator displacement assay, described in Chapter 1, was the paramount assay for these potential sensors. Since the maximum amount of dye displacement depends on the amount of metal chelation, which depends on the ligand, dendrimer, linker, and foundation, the indicator displacement assay shows how well the ensemble was synthesized as a complete entity.

3.2 CPG-CDI-G_{3,4}-terpy-Cu

This synthesis used CDI as a bi-functional linker between the CPG and PAMAM dendrimers of generations 3 and 4. The ligand, A-terpy, served as the chelate for copper ions, which created an exchangeable binding site for the indicator displacement assays. Holyer *et al.* observed the kinetic formation rate of Cu (II) bound to terpyridine to be $2 \times 10^7 \text{ mol}^{-1}\text{s}^{-1}$ for a mono complex.¹ Since the terpy-Cu binding was strong, it served as a stable end to the chemosensor.

3.2.1 CDI Coupled to CPG

The CDI assay, described in Chapter 2, was performed to quantify CDI activation at the CPG surface. The assay released imidazole and a calibration curve of Absorbance at 208 nm vs. [Imidazole] (Figure 3-1), produced by adding a 0.1 M imidazole solution into a 2.0 mL solution of pH 7.0 HEPES buffer, allowed the quantification of CDI.

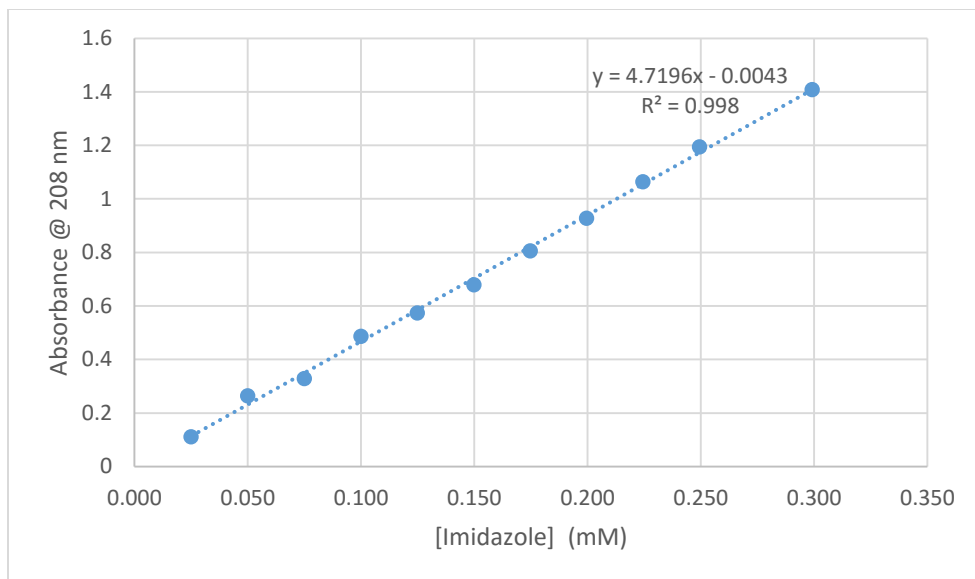


Figure 3-1. Typical calibration curve of Absorbance at 208 nm vs. free [Imidazole] in 5mM sodium phosphate dibasic buffer at pH 10.0 for imidazole release assay on the CPG surface.

Table 3-1 summarizes the results of four trials of the imidazole release assay showing the mass, absorbance at 208 nm, and conversion of released [imidazole].

Table 3-1. CPG-CDI assay results for the CPG-CDI-G_{3,4}-terpy-Cu ensembles

Sample	Mass (g)	Absorbance	Mol Imidazole / g CPG	μmol Imidazole / g CPG
CPG-CDI A	0.03321	0.626410	6.036E-05	60.36
CPG-CDI B	0.03209	0.574065	5.728E-05	57.29
CPG-CDI C	0.03139	0.557965	5.693E-05	56.93
CPG-CDI D	0.03090	0.555700	5.760E-05	57.60
				58 ± 2

Assuming a complete reaction, an average of 58 ± 2 μmol of imidazole per gram CPG means that there is good precision among the four trails (3.4 % RSD), where 58 μmol imidazole/g CPG is enough CDI to perform dendrimer reactions. Sandy Liu reported a comparable result during a CDI assay where she obtained a value of 60 μmol / g CPG.²

3.2.2 PAMAM Dendrimer Reactions to CPG-CDI

The CPG-CDI samples reacted with dendrimers of generation 3 and 4 to yield the dendrimer coated precursors CPG-G₃ and CPG-G₄. The dendrimers were redissolved into DMSO and all the reagents were mixed in a vial with N₂. Once the reaction completed, the products were washed, dried, and stored in a desiccator. A calibration curve of Absorbance at 268 nm vs. 4-NB Concentration (Figure 3-2), produced from the data obtained from adding a 0.1 mM 4-NB solution into a 2.0 mL solution of 0.2 % (v:v) acetic acid, allowed for the quantification of amines.

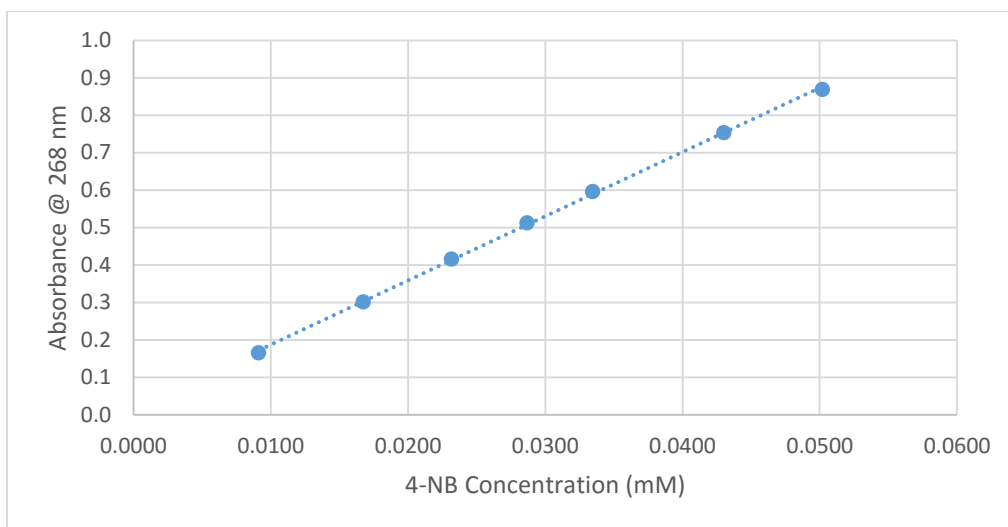


Figure 3-2. Typical calibration curve of Absorbance at 268 nm vs. 4-NB Concentration in a 0.2% acetic acid solution for amine density assay on the CPG-G_{3,4} precursors.

The amine assay, described in Chapter 2, leads to the results below in Table 3-2.

Table 3-2. Amine assay results for the CPG-CDI-G_{3,4} precursors

Sample	Mass (g)	Absorbance	Mol NH ₂ /g CPG	μMol NH ₂ /g CPG
CPG-G ₃ A	0.01047	0.028015	6.803E-07	0.6803
CPG-G ₃ B	0.01052	0.035498	1.091E-06	1.091
				0.9 ± 0.3
CPG-G ₄ A	0.01090	0.10304	4.667E-06	4.667
CPG-G ₄ B	0.01028	0.10716	5.182E-06	5.182
CPG-G ₄ C	0.01051	0.097161	4.514E-06	4.514
				4.8 ± 0.4

The prediction of a doubling of amines going from G₃ to G₄ (which also doubles the terminal amines) is not confirmed by the obtained data. The CPG-G₃ samples give 0.9 ± 0.3 μmol NH₂ per gram of CPG, whereas the higher generation CPG-G₄ samples give 4.8 ± 0.4 μmol NH₂ per gram of CPG. This ratio is about 5:1, not 2:1 as predicted. Although the amine density assay shows an increasing amount of amine groups as dendrimer generation increases, the absorbances for 10 mg samples are relatively low. Typical amine density assays, in past experiments in this research

group, give absorbance values in a range from 0.5 to 1.0.² Three possible conclusions can be drawn about this amine assay. First, there is a possibility that very few dendrimers reacted at the CPG-CDI surface, perhaps due to steric crowding, causing the low amine density assay results. The second possibility is a mistake in the assay that would result in low amine density. The third possibility is that the reactants could have degraded. Since the synthesis of each ensemble builds upon the previous steps, it will become clear if a mistake in the assay is the cause.

3.2.3 CDI Activation of CPG-G_{3,4}

Another CDI activation step added an electrophilic carbon monolayer to the dendrimer, which allowed for ligand reaction. Like the first CDI addition, a 20-fold excess of CDI added to each vial ensures maximum reaction to the dendrimer monolayer. Since many terminal amines coupled to the CPG-CDI particles during the dendrimer reactions, the dendritic primary amines were available for reaction with CDI. Therefore, the CDI assay on dendrimer modified CPG-CDI particles should give a higher number of CDI / g CPG than CPG-CDI particles. The CDI assay after dendrimer addition lead to the results in Table 3-3.

Table 3-3. CDI assay results for the activation of CPG-CDI-G_{3,4} precursors

Sample	Mass (g)	Absorbance	Mol CDI/g CPG	μMol CDI/g CPG
CPG-G ₃ -CDI A	0.01389	0.50140	1.175E-04	117.5
CPG-G ₃ -CDI B	0.01255	0.45432	1.180E-04	118.0
CPG-G ₃ -CDI C	0.01155	0.39069	1.104E-04	110.4
CPG-G ₃ -CDI D	0.01098	0.37833	1.125E-04	112.5
				115 ± 4
CPG-G ₄ -CDI A	0.01400	0.80697	1.871E-04	187.1
CPG-G ₄ -CDI B	0.01292	0.74418	1.870E-04	187.0
CPG-G ₄ -CDI C	0.01163	0.66657	1.862E-04	186.2
CPG-G ₄ -CDI D	0.01073	0.57490	1.743E-04	174.3
				184 ± 6

Compared to the CPG-CDI particle data in Table 3-1, the CPG-G_{3,4}-CDI particles (Table 3-3) have more bound CDI than the CDI saturated CPG. The ratio of the average values of CDI / g CPG between the G₄ and G₃ precursors is about 1.6 whereas the ratio of primary amines between G₄ and G₃ dendrimers is 2.0. The reason the average CDI / g values are lower than the maximum potential addition is because, upon binding, the dendrimers flatten which leave some of the primary amines inaccessible to the assay.³ Because of the higher CDI numbers and the G₄ / G₃ ratios for the second CDI assay, it is most likely that the amine assay was executed incorrectly, causing low absorbances. It was concluded that the dendrimer reaction did not fail, so the CPG-G_x-CDI activated precursors was reacted with the ligand, A-terpy.

3.2.4 A-terpyridine Activation of CPG-G_{3,4}

A-terpy was synthesized as described in Chapter 2 and is drawn in Figure 3-3.

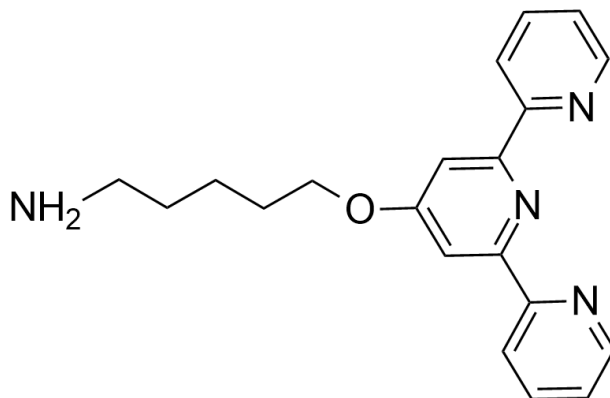


Figure 3-3. Aminofunctionalized-terpyridine ligand

To couple A-terpy to the surface, a large excess was added to the CPG-G_{3,4}-CDI precursors with triethylamine (TEA) and N-hydroxysuccinimide (NHS).⁴ The TEA acts as a base in the reaction

while NHS forms an intermediate that replaces the carboxylic acid (Figure 3-4) before the A-terpy couples to the precursor.

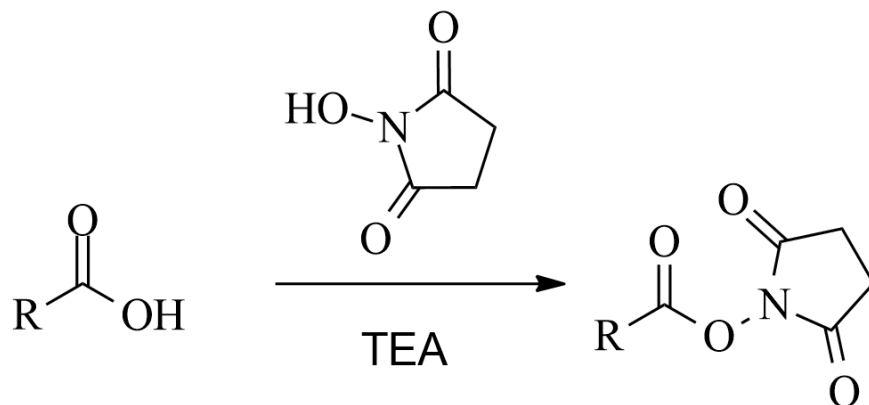


Figure 3-4. A carboxylic acid reacting with NHS to form an intermediate capable of nucleophilic substitution.

The reaction with A-terpy proceeded for 72 hours in an inert atmosphere before it was washed with dry methanol and filtered. Figure 3-5 shows a generic picture of this product.

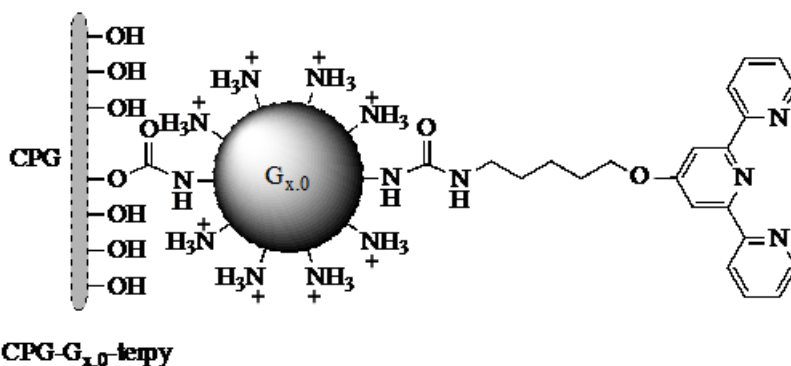


Figure 3-5. CPG-G_{x.0}-terpy linked via CDI activation of CPG.² The unreacted amines are in the acidic NH₃⁺ form.

The resulting CPG-G₃₋₄-terpy molecules were stored in a desiccator before the copper ions were loaded onto the ensemble.

3.2.5 Copper Loading onto CPG-G_{3,4}-terpy Precursors

Copper ions were loaded onto the precursors by flowing a 5 ppm Cu²⁺ solution through the ensemble in a short, packed column so the chelation site could bind to the copper ions. The effluent was collected dropwise, and after 280 drops (≈8.5 mL) a new test tube switched into place. These test tubes were analyzed by Atomic Absorption Spectrometry (AAS) to determine the copper ion concentration. As copper ions bind to the precursors, the Cu²⁺ effluent will decrease in concentration until all the copper ions chelate to the precursors. At this point, the chelation sites are saturated and the copper ions stay in solution raising the effluent concentration to the initial value. In the case of CPG-G_{3,4}-terpy, there was full binding of copper throughout the first 5 and 7 test tubes, respectively. Figure 3-6 shows the resulting breakthrough curves.

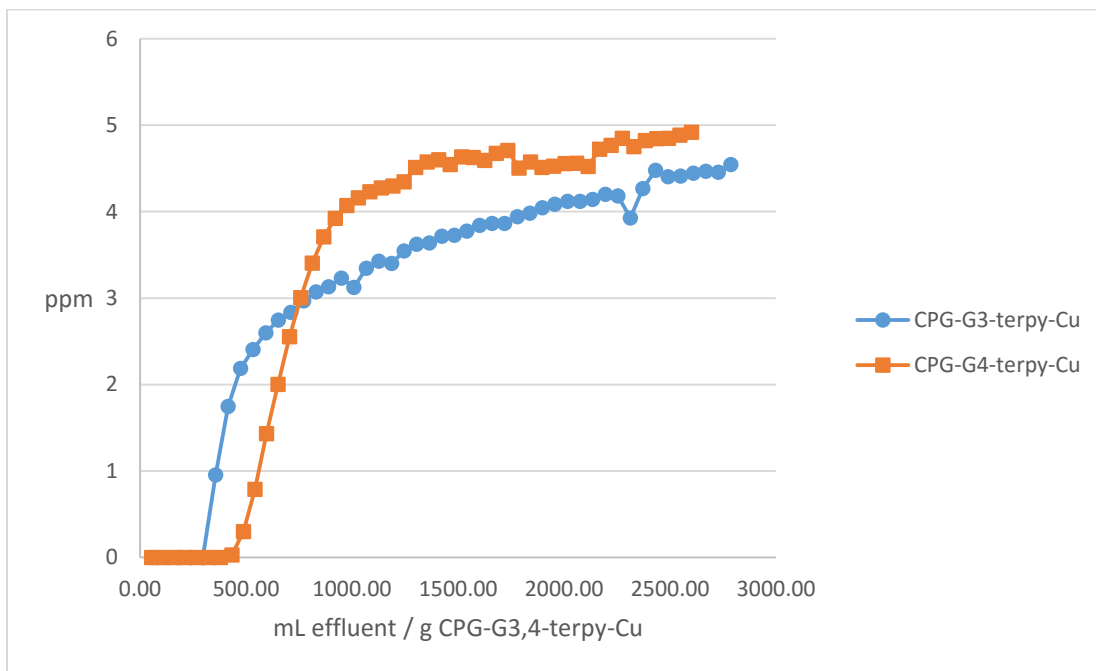


Figure 3-6. Breakthrough curve of CPG-G_{3,4}-terpy-Cu ensembles from the copper loading experiment. Each data point represents a test tube's copper ion concentration via AAS. The initial copper solution is 5 ppm Cu²⁺ in pH 7.0 ammonium acetate buffer.

Based on the data, the CPG-G₃-terpy-Cu required less effluent / g CPG than CPG-G₄-terpy-Cu to saturate with copper. Since the higher generation dendrimer has more terminal amines sites for A-terpy, CPG-G₄-terpy-Cu should have more bound copper than CPG-G₃-terpy-Cu. Table 3-4 shows the numerical analysis of the copper loading.

Table 3-4. Copper loading values for the CPG-G_{3,4}-terpy molecules.

Sample	Mass of Sample	Bound Copper (mg)	mmol Cu / g CPG
CPG-G ₃ -terpy-Cu	0.15213	20.84	2.156
CPG-G ₄ -terpy-Cu	0.15835	23.10	2.295

Even though the G₄ ensemble had more bound copper than the G₃ ensemble, the ratio of G₄:G₃ is only 1.1, which is much less than the 1.6 ratio calculated from the CDI assay. One possible reason for this discrepancy is that the copper ion concentration of the G₃ ensemble failed to level out. Since the amount of copper loaded on the ensemble was calculated by taking the difference of the initial copper solution concentration and the measured effluent concentration, the G₃ ensemble probably has less copper than the calculated value. If the copper ion concentration of the G₃ ensemble leveled out between 3 and 4 ppm, the ratio probably would have resembled the CDI assay ratio. The chelation of copper ions onto these two ensembles allowed for the indicator displacement assay to be performed.

3.2.6 Indicator Displacement Assays for CPG-G_{3,4}-terpy-Cu

The biological molecules L-histidine, L-leucine, L-alanine, and dopamine were used as substrates for the IDAs with the CPG-G_{3,4}-terpy-Cu chemosensors described in Chapter 2. For the IDA, four vials that contained CPG-G₃-terpy-Cu and four vials that contained CPG-G_{3,4}-terpy-Cu were shaken in dye solution for 24 hours. After 24 hours, the dye solution in each vial was

measured via UV-Vis to determine if the dye was binding to the chemosensor. Table 3-5 shows the results of the dye uptake step.

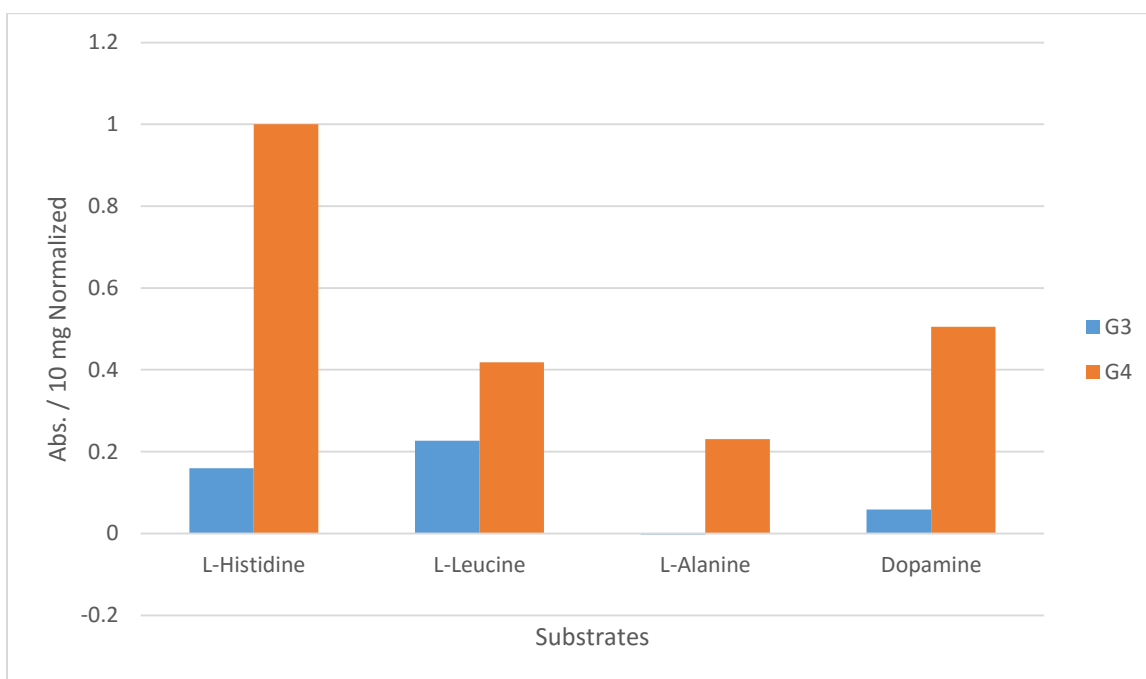
Table 3-5. PV dye binding absorbance values at 433 nm for CPG-G_{3,4}-terpy-Cu chemosensors before substrate addition

Trial Name	Mass of Chemosensor (g)	Δ Absorbance (Decline)	Δ Abs. / 10mg G_x-terpy-Cu
CPG-G ₃ -Terpy A	11.53	0.3588	0.3112
CPG-G ₄ -Terpy A	11.51	0.7010	0.6090
CPG-G ₃ -Terpy B	12.25	0.2741	0.2237
CPG-G ₄ -Terpy B	12.36	0.5848	0.4731
CPG-G ₃ -Terpy C	10.52	0.4504	0.4281
CPG-G ₄ -Terpy C	10.47	0.8467	0.8087
CPG-G ₃ -Terpy D	11.35	0.4095	0.3608
CPG-G ₄ -Terpy D	11.23	0.7358	0.6552
Δ Abs. Avg. of G ₃		0.33 ± 0.09	
Δ Abs. Avg. of G ₄		0.7 ± 0.1	

The four vials containing G₃ dendrimer on the chemosensor have an average change in absorbance of 0.33 ± 0.09 per 10 mg, whereas the vials containing G₄ dendrimer on the chemosensors have an average change in absorbance of 0.7 ± 0.1 per 10 mg. This shows that before the substrate was added to the vials, G₄ dendrimer chemosensors were absorbing twice as much dye as the G₃ dendrimer ensembles. These vials were then spiked with 25.1 μL of a 100 mM substrate solution, and shook for an additional 24 hours before the final absorbances were taken. The results for the substrate addition, along with normalized substrate bar graphs are shown in Table 3-6, and Figure 3-7 respectively.

Table 3-6. PV dye displacement assay values for CPG-G_{3,4}-terpy-Cu after substrate addition

Trial Name	Substrate	Mass of Chemosensor (g)	Δ Absorbance (Increase)	$\Delta A / 10\text{mg G}_x\text{-terpy-Cu}$
CPG-G ₃ -Terpy A	L-histidine	11.53	0.03412	0.02959
CPG-G ₄ -Terpy A	L-histidine	11.51	0.21336	0.18537
CPG-G ₃ -Terpy B	L-leucine	12.25	0.05149	0.04203
CPG-G ₄ -Terpy B	L-leucine	12.36	0.09590	0.07759
CPG-G ₃ -Terpy C	L-alanine	10.52	-0.00050	-0.00047
CPG-G ₄ -Terpy C	L-alanine	10.47	0.04474	0.04273
CPG-G ₃ -Terpy D	Dopamine	11.35	0.01238	0.01091
CPG-G ₄ -Terpy D	Dopamine	11.23	0.09399	0.09370

**Figure 3-7.** Substrate dye displacement normalized to the G₄ L-histidine dye displacement value

All of the G₄ chemosensors had a higher change in absorbance than its G₃ counterpart chemosensors. This was expected since the CDI assay, amine assay, and copper loading all produced results that show a higher density of each monolayer per gram of ensemble. The substrate L-histidine has the highest increase in absorbance, whereas L-alanine has no increase in

absorbance, meaning L-histidine is the most effective of the four substrates at displacing PV. The trend of increasing dye displacement mirrors the work of Gorman et al. Gorman quantified the basicity of amino acids and of the three amino acids used as substrates in this research, alanine was the least basic, followed by leucine, while histidine was the most basic.⁵ Dopamine and PV share a catechol group as a chelation mechanism, which could explain why dopamine displaced the second most dye of the G₄ chemosensors.

3.3 CPG-TESPSA-G₃-NTA-Cu

The synthesis of CPG-TESPSA-G₃-NTA-Cu is the second and final synthesis in this thesis and differs from the first in two ways. The first was the use of the new linker TESPSA in place of CDI, and the second was the substitution of the A-terpy ligand for lysine-NTA.

3.3.1 TESPSA Coupling to CPG

The idea for linking TESPSA to CPG, and using it as the primary synthetic step in this synthesis, came from a coworker, Jonathan Liu. Liu was using TESPSA as a linker on silica nanoparticles, which have similar linking characteristics to CPG.⁶ As stated in Chapter 2, an oxygen atom on CPG bonds to the silicon atom in TESPSA, displacing an ethoxy group to finish the coupling as shown in Figure 3-8.

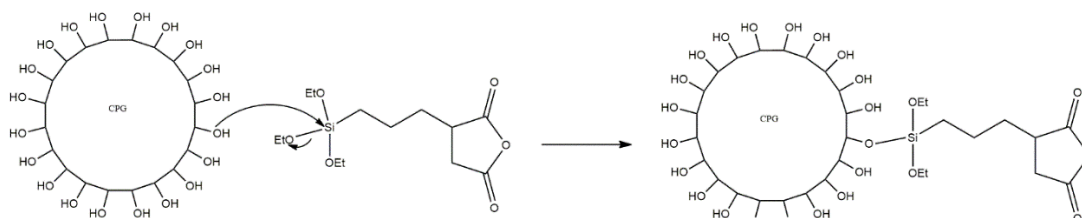


Figure 3-8. Nucleophilic substitution reaction between CPG and TESPSA

One disadvantage of using TESPSA over CDI is that there is no direct way to quantify the amount of TESPSA activated to CPG directly. This is a point of future research that will be

discussed later in Chapter 4. Although the concentration cannot be quantified directly, the success or failure of this synthesis can be seen in later quantifications of amine density, metal loading, and IDAs, as their values will be proportional to how well TESPSA couples to the CPG.

3.3.2 Dendrimer Modification of CPG-TESPSA

Only G₃ dendrimers were used with the TESPSA terminated ensemble in this experiment. The dendrimer addition reaction was performed under the same conditions as the CPG-G_{3,4}-terpy-Cu ensemble. As stated in Chapter 2, the amine density for the CPG-TESPSA-G₃ ensemble was 26 ± 2 $\mu\text{mol NH}_2$ per gram CPG before a buffer rinse and 59 ± 2 after a buffer rinse. Not only did the linker succeed in coupling the dendrimer, a new technique for activating terminal amines for this research was discovered as well.

3.3.3 CDI activation to CPG-TESPSA-G₃

The tethered dendrimer was activated by CDI so that a ligand could couple to the ensemble through a terminal carbonyl. Like the CDI additions in previous reactions, 20-fold excess of CDI was added to each reaction vial to ensure maximum adhesion to the dendrimer monolayer. After the reaction, the CDI assay on the ensemble gave the results shown in Table 3-7.

Table 3-7. CDI assay values for CPG-TESPSA-G₃-CDI

Sample	Mass (g)	Absorbance	Mol CDI / g CPG	$\mu\text{mol CDI /g CPG}$
CPG-TESPSA-G ₃ A	0.01383	0.99226	1.444E-06	104.4
CPG-TESPSA-G ₃ B	0.01504	1.00055	1.456E-06	96.80
CPG-TESPSA-G ₃ C	0.01748	1.02450	1.489E-06	85.19
				100 \pm 10

The average amount of activated CDI to the dendrimer layer was 100 ± 10 $\mu\text{mol CDI}$ per gram CPG. This value is slightly lower than using the usual CDI linker for tethering dendrimer to

CPG in the synthesis of the CPG-G_{3,4}-terpy-Cu chemosensor, which gave 115 ± 4 μmol CDI per gram CPG. However, since the values are comparable and the TESPSA provides a much longer tether, ligand activation reactions as well as a copper loading experiment were performed in order to test the effect of chelating tether distance upon the IDA.

3.3.4 Lysine-NTA Ligand Activation and Copper Loading to CPG-TESPSA-G₃

The ligand activation was performed under the same conditions as the CPG-G_{3,4}-terpy-Cu chemosensor; however, lysine-NTA was used instead of A-terpy (Figure 2.5). The copper loading experiment was carried out in the same way. During the AA analysis of the effluent Cu²⁺ solution, the absorbances for Cu²⁺ were double the concentration of the Cu²⁺ solution, which was not possible. There may have been an instrumentation error, but no reliable copper loading breakthrough curve or numerical analysis were produced. It was assumed that the copper loading still gave material useful for an IDA, so the resulting metal saturated chemosensor was analyzed via an IDA.

3.3.5 IDAs on CPG-TESPSA-G₃-NTA-Cu Chemosensors

The biological molecules L-histidine, L-leucine, L-alanine, and dopamine were used as substrates for the IDA. L-histidine was run in triplicate in this experiment to investigate repeatability. The IDA conditions were the same as for the CPG-G_{3,4}-Terpy-Cu chemosensors. Table 3-8 shows the results of the dye absorption step.

Table 3-8. PV dye binding assay values for CPG-TESPSA-G₃-NTA-Cu before substrate addition.

Trial Name	Mass of Beads (mg)	Δ Absorbance (Decline)	ΔA / 10mg G₃-NTA-Cu
CPG-TESPSA-G ₃ -NTA A	10.49	0.66364	0.63264
CPG-TESPSA-G ₃ -NTA B	10.63	0.67123	0.63145
CPG-TESPSA-G ₃ -NTA C	10.44	0.69063	0.66152
CPG-TESPSA-G ₃ -NTA D	10.29	0.69726	0.67761
CPG-TESPSA-G ₃ -NTA E	10.49	0.67594	0.64437
CPG-TESPSA-G ₃ -NTA F	10.71	0.67796	0.63302
Δ A Avg. of G₃			0.65 ± 0.02

These G₃ dendrimer chemosensors have an average change in absorbance of 0.65 ± 0.02 per 10 mg. This shows that before the substrate was added to the chemosensors, CPG-TESPSA-G₃-NTA-Cu chemosensors were absorbing twice as much dye as the CPG-G₃-terpy-Cu ensembles. Two possible reasons that the NTA chemosensor was absorbing more dye than the A-terpy chemosensor were the solubility of the ligands and/or better access for copper ions to the NTA binding sites due to the longer TESPSA linker. Terpy is much more hydrophobic than NTA.⁷ Since the IDA was performed in an aqueous environment, the hydrophilic NTA was more suitable in these conditions. The K_f of terpy metal binding is typically lower than the K_f of NTA metal binding.^{8,9} These vials were spiked with 25.1 μ L of a 100 mM substrate solution and shook for an additional 24 hours before their final absorbances were taken. The results for the substrate addition, along with normalized dye release values compared to CPG-G₃-terpy-Cu, are shown in Table 3-9 and Figure 3-9 respectively.

Table 3-9. PV dye displacement assay values for CPG-TESPSA-G₃-NTA-Cu after substrate addition

Trial Name	Substrate	Mass of Beads (mg)	Δ Absorbance (Increase)	$\Delta A / 10\text{mg G}_3\text{-NTA-Cu}$
CPG-TESPSA-G ₃ -NTA A	L-histidine A	10.49	0.09908	0.09445
CPG-TESPSA-G ₃ -NTA B	L-histidine B	10.63	0.09590	0.09022
CPG-TESPSA-G ₃ -NTA C	L-histidine C	10.44	0.08018	0.07680
CPG-TESPSA-G ₃ -NTA D	L-leucine	10.29	0.06413	0.06232
CPG-TESPSA-G ₃ -NTA E	L-alanine	10.49	0.04402	0.04196
CPG-TESPSA-G ₃ -NTA F	Dopamine	10.71	0.16449	0.15359

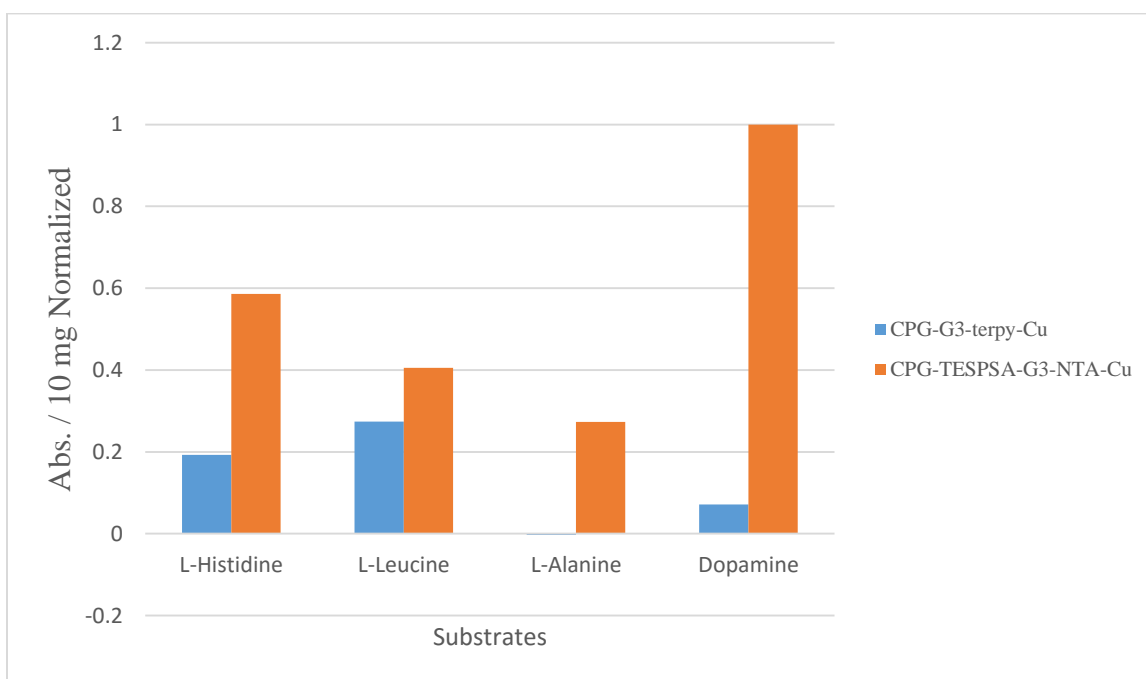


Figure 3-9. Substrate dye displacement normalized to the CPG-TESPSA-G₃-NTA-Cu dopamine dye displacement value

The L-histidine spiked samples show reasonable repeatability with an average of $0.09 \pm 0.01 \Delta A / 10 \text{ mg G}_3\text{-NTA-Cu}$. Dopamine has the highest increase in absorbance whereas L-alanine has the least increase in absorbance meaning that dopamine is the most selective of the four

substrates. Of the three amino acids, the same trend is seen where the more basic the amino acid, the more dye displaced. The dye displacement values for CPG-TEPSA-G₃-NTA-Cu are all higher than the CPG-G₃-terpy-Cu values. Since there are two different variables between these chemosensors, it is difficult to determine if these increases are because of the NTA ligand, the TEPSA linker, or a combination of the two. In future experiments, chemosensors should be created with only one synthetic difference to determine which of the three possibilities is true.

3.4 Conclusion

Three distinct chemosensors, CPG-G_{3,4}-terpy-Cu and CPG-TEPSA-G₃-NTA-Cu, were synthesized and characterized before conducting IDA assays using PV binding and displacement for a series of biologically important substrates. In the case of CPG-G_{3,4}-terpy-Cu, the G₄ dendrimer had twice the dye absorption compared to its G₃ counterpart, which was expected because the G₄ dendrimers have more terminal amine sites. The TEPSA molecule was used as the linker on the CPG-G₃-NTA-Cu ensemble. The CDI assay showed that the TEPSA linked G₃ dendrimer had similar amounts of CDI on the ensemble, after dendrimer addition, to the original CDI linked ensemble. The CDI linked ensemble had $115 \pm 4 \mu\text{mol CDI} / \text{g CPG}$ compared to $100 \pm 10 \mu\text{mol CDI} / \text{g CPG}$ for the TEPSA linked ensemble. However, in the IDAs, the TEPSA linked chemosensor had higher dye absorption as well as higher dye displacement. It is difficult to make a direct comparison here because of the different ligands used in each synthesis, yet the differences in dye binding and displacement by substrates was dramatically better. This is a key preliminary discovery in that the data imply that a combination of the longer TEPSA linker and the NTA chelate gave much larger response than the CDI-linked G₃ terpy ensemble. One can imagine that the TEPSA-G₃ sticks out further into solution exposing itself to better solvation or

chelation reactions giving higher loadings. This is one area of future research that needs to be explored.

3.5 References

1. Holyer, R. H.; Hubbard, C. D.; Kettle, S. F. A.; Wilkins, R. G., The Kinetics of Replacement Reactions of Complexes of the Transition Metals with 2,2',2''-Terpyridine. *Inorg. Chem.* **1966**, 5 (4), 622-625.
2. Liu, S., Synthesis and study of various functional surfaces generated on PAMAM dendrimers immobilized controlled pore glass. M.S. Thesis, University of San Francisco, San Francisco, CA. **2013**.
3. Fail, C. A., Evenson, S. A., Ward, L. J., Schofield, W. C. E., Badyal, J. P. S., Controlled Attachment of PAMAM Dendrimers to Solid Surfaces. *Langmuir* **2002**, 18, 264-268.
4. Jiang, K., Schadler, L. S., et al., Protein Immobilization on Carbon Nanotubes Via a Two-step Process of Diimide-activated Amidation. *J. Mater. Chem.* **2004**, 14, 37-39.
5. Gorman, G. S., Speir, J. P., Turner, C. A., Amster, I. J., Proton Affinities of the 20 Common α -Amino Acids. *J. Am. Chem. Soc.* **1992**, 114, 3986-3988.
6. Katur, V., Eichler, M., Deigle, E., et al., Surface-immobilized PAMAM-dendrimers modified with cationic or anionic terminal functions: Physicochemical surface properties and conformational changes after application of liquid interface stress. *J. Colloid Interface Sci.* **2012**, 366, 179-190.
7. *Chemspider*. February 24, 2016. www.chemspider.com.
8. Furia, Thomas E. *Crc Handbook of Food Additives*. 2nd ed. Vol. 1. Boca Raton, Florida: CRC, **1975**.
9. Shunmugan, R.; Gabriel, G.; Aamer, K; Tew, G; Metal-Ligand-Containing Polymers: Terpyridine as the Supramolecular Unit. *Macromol. Rapid Commun.* **2010**, 31, 784-793.

Chemosensor Optimization and Other Future Research Areas

4.1 Introduction

In this chapter, future research options are considered for CPG foundation chemosensors. One topic of future research is optimizing chemosensor properties. For example, if a chemosensor can absorb and release more dye per gram of CPG, substrates at lower concentrations can be quantified, leading to more sensitive measurements. One method to increase dye absorption and dye release would be to have more available metal sites on a chemosensor. An increase in metal sites on a chemosensor can be accomplished by optimizing each step of the synthesis leading up to the metal addition. Other future research areas include potential assay improvements along with qualitative spectroscopic techniques to prove linker coupling.

4.2 Synthesis and Assay Optimization

This section discusses where, in the synthesis of a chemosensor, optimizations and changes can be made to improve the sensitivity of the chemosensor along with other assay and spectroscopic improvements. Areas for chemosensor improvement include further optimization of the TESPSA linker chemistry, using larger dendrimer generations, testing the effect of HEPES buffer washing before synthetic steps, implementing different and more metal ion selective ligands, optimizing the competitive dye binding used in IDAs, and testing a variety of different substrates.

4.2.1 TESPSA Usage and Proof of Coupling

TESPSA and CDI were used in this research to couple the CPG foundation to a dendrimer. Although the TESPSA linker gave lower densities in the CDI assay compared to CDI as a linker

[TESPSA = 100 ± 10 μmol CDI per gram CPG, versus CDI = 115 ± 4 μmol CDI per gram CPG], more chemosensors should be synthesized with TESPSA to see if the linker could lead to higher metal loading values. This can be done by creating several CPG-CDI- $G_{x,y,z}$ -CDI-Linker-Cu batches along with several CPG-TESPSA- $G_{x,y,z}$ -CDI-Linker-Cu batches and plotting a breakthrough curve on all the batches. By comparing these ensembles side by side using different generation dendrimers, a better picture will emerge as to how well TESPSA links the dendrimer compared to CDI. If the results are comparable, the linker's experimental procedure, cost, and ease of use should be considered for choosing the most optimal linker.

Another future test using TESPSA is to characterize its coupling to CPG directly, and to obtain evidence of this coupling. The TESPSA linker should have spectroscopic differences in the FT-IR compared to a CPG sample. Since the acid washed foundation of CPG is made of silica with alcohol groups on its outer layer, an FT-IR spectrum wouldn't show any sp^2 or sp^3 hybridized carbon-hydrogen stretching or carbonyl stretching that a TESPSA monolayer on CPG should show.¹ FT-IR would be a quick and easy way to determine if the TESPSA reacts without having to synthesize an ensemble.

4.2.2 Dendrimer Generation Usage on Future Chemosensors

Since dendrimers of higher generation have twice as many terminal amines as previous generations,² they should react with more ligands and metal ions, thus increasing the amount of dye binding during the IDA assays. This should improve sensitivity since the amount of dye released per g CPG should be higher. The trend was observed for CPG- $G_{3,4}$ -terpy-Cu IDAs where the G_3 ensemble had a 0.33 ± 0.09 average change in absorbance versus the G_4 ensemble with 0.7 ± 0.1 average change in absorbance. Chemosensors should be created using dendrimers with

generations 5.0, 6.0 and even 7.0 to see if the generation jump induces a doubling effect throughout or if it slowly levels out. Higher generation dendrimers are much more expensive than lower generations, but are larger and possibly beneficial to put on a surface. By making chemosensors with higher generation dendrimers, an optimal balance can be found between dendrimer size and copper loading.

4.2.3 HEPES Buffer Washing

In Chapter 2, the results of two amine assays were discussed in which one assay was performed without a buffer wash, prior to the assay, and one was performed with a buffer wash. The samples that were not buffer washed yielded 26 ± 2 NH_2 per gram CPG while the ones that were buffer washed yielded 59 ± 2 NH_2 per gram CPG. Therefore, a pH 7.0 HEPES buffer wash on dendrimer modified CPG increased the availability of reactive dendrimer terminal amines on the CPG. The pH 7.0 HEPES buffer wash must have caused deprotonation of the positively charged terminal amine, which has a pK_a of 6.9,³ leaving the lone pair of valence electrons on the primary amine nitrogen. Since the nucleophilic terminal amines are critical to the success of subsequent reactions, buffer washes should be performed before nucleophilic reactions on chemosensors to ensure the maximum amount of linker is coupled to the dendrimer. When the synthesis of a chemosensor reaches the IDA step, the chemosensor will be more efficient because of higher chelate-metal loadings.

4.2.4 Ligand Diversity

Metal ion chemosensors need a metal ion chelating ligand with a linker that reacts with the dendrimer. Lysine-NTA and A-terpy both have these properties. One area of future research would be to find or synthesize compounds that have these properties but may have different

hydrophobic properties, metal ion selectivity, or possess more open coordination sites for dye/substrate exchange reactions. An aminofunctionalized 2,2'-bipyridine, A-bipy, molecule could be used as a future ligand on chemosensors (Figure 4-1).⁴

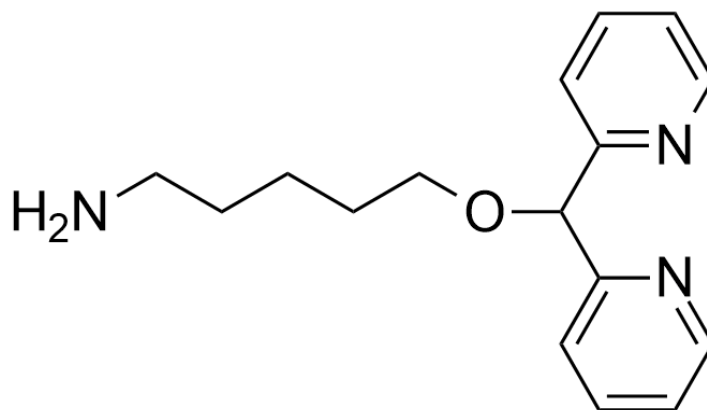


Figure 4-1. A-bipy molecule that can be used as a potential ligand.

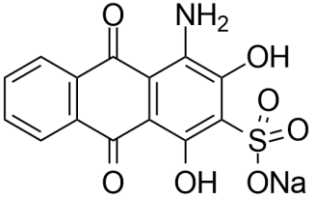
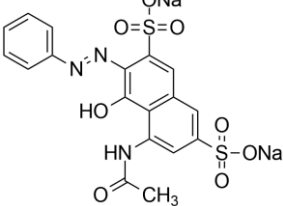
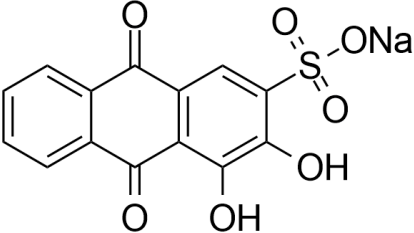
One possible advantage of a ligand like A-bipy is that a metal ion can be strongly bound by the two aromatic nitrogen leaving three or more open sites for unique dyes and substrates to bind. By creating and coupling new chelating ligands to these chemosensors, the IDA will change to become more selective or more effective with matching dyes or substrates.

4.2.5 Dye Optimization

Pyrocatechol violet used as the metal ion binding dye in this research has a tendency to decompose over time, especially when exposed to light. Careful measures were taken during IDAs to make sure that only minimal amounts of light reached the vials containing PV. The vials were wrapped in aluminum foil and then surrounded by paper towels during the two 24 hour shaking periods. In addition, the vials were only unwrapped during the UV-Vis measurement. Finding a dye less sensitive to light while having the same binding properties of PV would make the assay execution easier and eliminate dye degradation issues. Substitute dyes

that could be used in an IDA include: Nuclear Fast Red, Azophloxine, and Alizarin Red S (Table 4-1). Nuclear fast red has hydroxyl and amino groups and has been used to chelate numerous metal ions for chemical analysis.⁵ Azophloxine, which has been used to selectively detect histidine containing peptides,⁶ also uses hydroxyl and amino groups to chelate metals but the chelation forms a 6 member ring as opposed to nuclear fast red which forms 5 a member ring. Lastly, Alizarin Red S, which has been used in a copper ensemble to detect glutathione,⁷ is similar to PV as it has a catechol group available for chelating metal ions.

Table 4-1. Names and structures of new dyes to test for IDAs.⁸

Dye Name	Structure
Nuclear fast red	 <p>The structure of Nuclear fast red consists of a central benzene ring fused to a naphthalene-like system. It features a primary amine group (-NH₂) and two hydroxyl groups (-OH) on the benzene ring, and a sulfonate group (-SO₃Na) also on the benzene ring. Two carbonyl groups (=O) are attached to the naphthalene system.</p>
Azophloxine	 <p>The structure of Azophloxine features a central benzene ring with a phenyl ring attached via an azo group (-N=N-). It also has a hydroxyl group (-OH), an acetamido group (-NHCOCH₃), and a sulfonate group (-SO₃Na) on the benzene ring. A sodium ion (Na⁺) is shown near the sulfonate group.</p>
Alizarin Red S	 <p>The structure of Alizarin Red S is similar to Nuclear fast red, with a central benzene ring fused to a naphthalene-like system. It features two hydroxyl groups (-OH) on the benzene ring and a sulfonate group (-SO₃Na) also on the benzene ring. Two carbonyl groups (=O) are attached to the naphthalene system.</p>

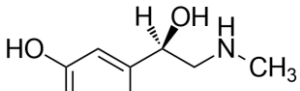
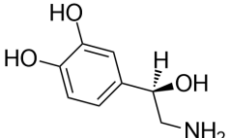
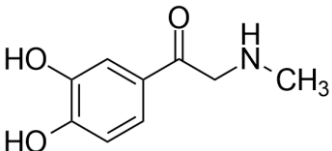
Since these structures differ in their size and chelation site chemistry, performing an IDA with these three compounds could produce a more durable dye than PV. By testing these compounds

as IDA dyes, the metal ion binding ability, the substrate displacement, and decomposition rates can be compared to each other to determine which dye has the properties most suitable for an IDA.

4.2.6 Additional Substrates for IDAs

The entire purpose of the chemosensor is to quantify substrates in a solution. Therefore, vast numbers of substrates could be selected by rational design based upon structural binding to open metal ion coordination sites and tested to get binding properties and see how they perform in an IDA. By looking at the data for the amino acid substrates, one can see that even though the molecules have the same binding chemistry and only different R-groups, the molecules should have different binding affinities to chelated copper ions on NTA and A-terpy chemosensors. For future research, additional amino acids should be tested along with other catechol-like molecules such as epinephrine, norepinephrine, and adrenalone. These molecules along with other catecholamines have already been the focus of biological sensors.^{9,10} The structures of these catechol containing molecules (which should bind to a chelated copper complex at the 1,2 hydroxyl groups) are shown below in Table 4-2.

Table 4-2. Names and structures of new substrates to test in IDAs.⁸

Substrate Name	Structure
Epinephrine	
Norepinephrine	
Adrenalone	

Along with the previous substrates analyzed in this work, obtaining data for these biologically important molecules would show the versatility of chemosensors and provide information on these molecules.

4.3 Conclusions

In conclusion, there are many ways to improve these chemosensors by optimization of existing methods and new rational design. The linker TESPSA chemistry requires more experiment to determine whether it could be more useful than CDI. Dendrimer generations above 5.0 could be used to see if there is a limit to how many more terminal amines can be added to the CPG surface. The research question is “Will the density of terminal amines quantified in the amine density assay increase with each increase in generation, or would the amount of terminal amines level off?” HEPES pH 7.0 buffer washes activate more terminal amines via deprotonations, but more experiments would confirm this step. In addition, designing a ligand with a good nucleophilic linker on one end while having strong metal ion chelation properties on the other side could improve loading and metal binding selectivity to the chemosensor. Experimenting with new dyes like Nuclear Fast Red, Azophloxine, and Alizarin Red S could produce a more resilient dye, with different metal ion binding properties, making IDAs exchange differently with different substrates and different spectroscopic properties. Lastly, a well-designed geometry specific chemosensor could selectively bind certain substrates over others based on facial or meridian geometry preferences. Geometry specific substrates can be selected

that displace the dye from the binding site on the metal complex. This could produce a selective IDA for biologically important molecules from amino acids to neurotransmitters.

4.4 References

1. Carey, F. *Organic Chemistry*. 7 ed. **2008**, New York, New York: The McGraw-Hill Companies, Inc.
2. Liu, S., Synthesis and study of various functional surfaces generated on PAMAM dendrimers immobilized controlled pore glass. M.S. Thesis, University of San Francisco, San Francisco, CA. **2013**.
3. Haensler, J.; Szoka Jr., F., "Polyamidoamine Cascade Polymers Mediate Efficient Transfection of Cells in Culture." *Bioconjugate Chem.* **1993**, 4, 372-378.
4. Kiss, T., Gergely, A., "Copper(II) and Nickel(II) Ternary Complexes of L-Dopa and Related Compounds." *J. Inorg. Biochem.* **1985**, 4, 247-259.
5. Gholivand, M. B., Romiani, A. A., "Application of Adsorptive Stripping Voltammetry to the Simultaneous Determination of Bismuth and Copper in the Presence of Nuclear Fast Red." *Anal. Chim. Acta.* **2006**, 571, 99-104.
6. Buryak, A., Severin, K., "An Organometallic Chemosensor for the Sequence-Selective Detection of Histidine- and Methionine-Containing Peptides in Water at Neutral pH." *Angew. Chem. Int. Ed.* **2004**, 43, 4771-4774.
7. Chen, Z. et al, "Alizarin Red S/Copper Ion-based Ensemble for Fluorescence Turn on Detection of Glutathione with Tunable Dynamic Range." *Biosensors and Bioelectronics.* **2012**, 202-208.
8. *Sigma Aldrich*. June 12, 2014. www.sigmaaldrich.com.
9. Szeponik, J. et al, "Ultrasensitive Bienenzyme Sensor for Adrenaline." *Biosensors and Bioelectronics.* **1997**, 12, 947-952.
10. Lisdat, F. et al, "Catecholamine Detection Using Enzymatic Amplification." *Biosensors and Bioelectronics.* **1997**, 12, 1199-1211.